UAV RGB images to assess the seasonal effect of canopy on accuracy of DTM and Forest AGB/carbon estimation in Haagse Bos Netherlands.

WOINSHET WORKU

June, 2020

SUPERVISORS:
Dr. Y.A. Hussin
Ir L.M. van Leeuwen – de- Leeuw

UAV RGB images to assess the seasonal effect of canopy on accuracy of DTM and Forest AGB/carbon estimation in Haagse Bos Netherlands.

WOINSHET WORKU

Enschede, The Neatherlands, June, 2020

Thesis submitted to the Faculty of Geo-Information Science and Earth Observation of the University of Twente in partial fulfilment of the requirements for the degree of Master of Science in Geo-information Science and Earth Observation.
Specialization: Natural Resources Management

SUPERVISORS:
Dr. Y.A.Hussin
Ir.L.M.van Leewen-de-Leeuw

THESIS ASSESSMENT BOARD:

Dr.Ir.C.A.J.M.de Bie (Chair)
Dr. T. Kauranne (External Examiner, LUT School of Engineering Science, Finland)

ABSTRACT

Light Detection and Ranging technology (Lidar) is a survey tool used for several applications in the field of forestry and forest research. It used to capture the 3D structure of topography and vegetation accurately and quickly cover large areas. Lidar can model the vertical distribution of the canopy and ground surface, which will give full information about vegetation structure, and it estimates the tree crown size, tree height, basal area and stem volume accurately. However, the data set obtained from airborne Lidar is costly to use for regular monitoring and not always accessible. Recently the emerging technology of Unmanned Aerial Vehicle (UAV) is becoming operational in various purposes and applications. This platform is operated from the ground and provide a promising way for timely and cost-effective monitoring of environmental phenomena and natural resources at a very high spatial and temporal resolutions.

The major objective of this paper was to assess the seasonal effect of the canopy on the derived DTM, CHM and the outcome of AGB. Thus UAV photogrammetric images captured during the leaf-on and leaf-off season were analysed and assessed how they influence the result. The accuracy of results was evaluated taking Lidar as reference.

In this study, the accuracy of DTM generated from UAV RGB images of leaf-on and leaf-off seasons was assessed compared to Lidar derived DTM. The result obtained indicates that the accuracy of DTM from UAV images of the leaf-off season was comparable with the Lidar derived DTM and showed a strong correlation. The RMSE error of leaf-off season was 0.25. But, the accuracy of DTM during the leaf-on season was declined, and an error increased to 0.3. The UAV leaf-on and leaf-off seasons DTM has 80% and 72% correlation with reference DTM, respectively.

The comparison of tree heights extracted from UAV RGB images of leaf-on and leaf-off season has shown a strong correlation with RMSE and R^2 of 2.2 m and 0.88, which show that tree height measurements explain 88 % of the difference in height measurement in UAV leaf-on season from leaf-off season data. Similarly, the AGB/AGC computed from UAV leaf-on and leaf-off season has good agreement with each other and resulted R^2 of 0.96 with RMSE of 0.13 and 0.06 Mg/tree respectively.

The accuracy assessment of AGB derived from Lidar and UAV datasets has shown a positive and strong correlation. The comparison of Lidar AGB with UAV leaf-on season has shown R^2 of 0.85 with RMSE of 0.724 Mg/tree. Whereas, UAV leaf-off season has shown R^2 and RMSE of 0.91 and 0.72 Mg/tree respectively.

Keywords: leaf-on; leaf-off; Height; UAV; AGB; DTM; CHM; Lidar

ACKNOWLEDGEMENTS

First of all, I would like to express my deepest gratitude and appreciation to Almighty God for making things to happen according to his will. Thank you for giving me a way to pass through different challenges; for guiding and strengthening me; for keeping me safe and healthy.

My most enormous thanks goes to Nuffic's Orange Knowledge Programme (OKP) for offering me this scholarship opportunity to pursue this MSc. Degree. I thank you for all financial and other related supports giving me throughout my study time.

I take this chance to thank my first supervisor Dr. Yousif Hussin, for your valuable comments and follow up starting from proposal to final stage of the research work. I thank you for your patience and tolerance, and I am grateful for your togetherness during our challenging fieldwork time in Thailand. I would also like to thank my second supervisor Ir. LM van Leeuwen – de Leeuw, for your constructive comments and ideas throughout the research work.

I am also sincerely grateful to our mentor and NRM course director, Drs. R.G.Nijmeijer for your advice, support; ideas and valuable discussion during course study time. I am very thankful to my chairperson dr.ir.C.A.J.M.de Bie for your ideas on drafting the conceptual diagrams and helpful and encouraging words. I would like to thank the whole NRS family and teaching staffs for the knowledge and experience you shared with us.

My deepest thanks also goes to my families, Mom, dad and siblings. Thank you for your prayers, moral support, encouragement and love.

I would like to extend thanks to my brother dr. Abebe Demise Chukalla for giving me scholarship information and for helping and guiding me throughout all application process. To my friend Meron Eshatae for your support, encouragement and true love. Thank you for being with me with all ups and downs.

Finally, I like to thank all my NRM fellow students, friends and others who contributes something in one or other way.

TABLE OF CONTENTS

LIST OF FIGURES

LIST OF TABLES

LIST OF EQUATIONS

LIST OF APPENDICES

LIST OF ACRONYMS

AAT	Automatic Aerial Triangulation
AGB	Above Ground Biomass
AGC	Aboveground carbon
AHN	Actueel Hoogtebestand Netherlands
BBA	Bundle Block Adjustment
BEF	Biomass expansion factor
CD	Crown Diameter
CF	Conversion factor
CHM	Canopy Height Model
Cm	Centimetre
CO2	Carbon dioxide
CP	Checkpoint
CPA	Crown projection area
DBH	Diameter at breast height
DSM	Digital Surface Model
DTM	Digital Terrain Model
FAO	Food and Agriculture Organization
GCP	Ground control points
GHG	Green House Gas
GIS	Geographic Information System
GNSS	Global navigation satellite system
GPS	Global Positioning System
GSD	Ground resolution distance
Gt	Gigatons
IMU	Inertial measurement unit
IPCC	Intergovernmental Panel on Climate Change
LiDAR	Light Detection and Ranging
Mg	Megagram
RADAR	Radio Detection and Ranging
RMSE	Root Mean Square Error
RS	Remote Sensing
SAR	Synthetic Aperture Radar
SfM	Structure from Motion

UAV	Unmanned Aerial Vehicle
UNFCCC	United Nations Framework Convention on Climate Change
3D	Three Dimensional
2D	Two Dimensional

1. INTRODUCTION

1.1. Background and Justification

Our planet has a variety of forest types, which includes wintry boreal forests, the colourful temperate deciduous forests, humid temperate evergreen forests as well as diverse tropical forests and some others (Vankat, 2002). The tropical forest covers 47% of the world's forest, which is the highest compared to the temperate and boreal forest. Whereas the sub-tropical, temperate and boreal forests cover 9%, 22% and 33% of the worlds forest respectively (European Commission, 2003). Temperate forests are grown in the mid-latitudes, from the Tropic of Cancer (23½º north latitude) to 50º North latitude, and at the South of the tropic of Capricorn (23½º south latitude) (Gorte & Sheikh, 2010). Temperate forests primarily grow in areas of North America, West and Central Europe, North-eastern Asia, New Zealand, Southern Chile, and the Mediterranean. The temperate ecosystem includes a variety of vegetation with different kinds of species (Lal et al., 2012). It comprises different vegetation types, including hardwood vegetations like Oak, Beech and Birch species, as well as softwood trees of Pine, Douglas-fir and spruce species and some mixed vegetation types like Oak-Pine. However, compared to the tropical forest, the temperate forest ecosystem has less tree species diversity (Gorte, 2009).

The temperate forests represent one of the leading ecosystems on earth. In terms of area coverage, the temperate forest accounts for almost 22% of the global forests and earth's terrestrial land surface(de Gouvenain & Silander, 2017). Temperate forests are as one of the dominant forest types along with the boreal, tropical/ subtropical dry and wet forests. Compared to the other types of forests, temperate forests are intermediate in terms of temperature, latitude, and precipitation (Dreiss & Volin, 2014). The temperate forest ecosystem has four different seasons, which is summer, autumn(fall), winter and spring. The summer season has more daylight hours compared to the other seasons, and the maximum temperature will reach up to 30°C. Majority of the deciduous trees of temperate forest drop their leave during the fall (autumn) season. Its lower temperature characterises winter season, and the minimum may reach to -30°C. The temperate forest vegetation re-grow and bloom during the spring season (Lal et al., 2012).

Temperate forests provide a wide arrange of ecosystem services and goods globally, regionally, and locally. It holds the oldest and most abundant organisms in the world. It is also one of the world's primary source of wood and timber production as well as it is the only forest which has potential for sustainable forest management (de Gouvenain & Silander, 2017). Temperate forests play a vital role in watershed management, protection and soil stabilisation (Newton & Featherstone, 2005). It also used as the source of food, wood for construction, firewood, and source of oxygen for all life on earth. These forests serve as the lungs of the planet, because of their ability and potential to capture and store carbon; and produce oxygen (Paulista et al., 2010). Even so, most of the temperate forests managed for commercial wood products; the management practices used in this forest can have a substantial effect on the process of carbon sequestration (Gorte, 2009).

Temperate forests store carbon which released from both industrial and anthropogenic activities. They are crucial in regulating nitrogen, hydrological, and carbon cycles (de Gouvenain & Silander, 2017). The total carbon pool of temperate forest is estimated around 100 Gt (gigatons) (Potapov, 2009); this number is very close with the number given by (Heath et al., 1993) which is 98.8 Gt (gigatons) and each temperate forest are assumed to contain up to 57.1 tonnes of carbon per ha in living vegetations. The figure is lower than the boreal and the tropical forests, but it has a very significant role in climate change mitigation. Temperate forests in Europe are estimated to store on average form 7% to 12% of all carbon released from human activities (anthropogenic emissions). The amount of carbon stock is higher in Nordic regions compared to the other. The Nordic regions have the highest forest coverage and account for 25 to 50 tonnes of carbon per hectare; whereas the Mediterranean regions store 5 to 25 t/ha (Federal Reasearch Centre for Forestry and, 2006).

Different kinds of remote sensing techniques can be used to assess and estimate forest above-ground biomass (AGB)/carbon. Some of the previous studies used optical remote sensing data which ranges from high to low spatial resolutions: IKONOS, Quick bird, Worldview, SPOT, Sentinel, Landsat and MODIS(Kumar & Mutanga, 2017). Other applied radar remote sensing data for AGB/carbon estimation, because of its ability to penetrate the cloud and complete vegetation structure information. Currently, different types of radar remote sensing data have been available for various purposes. These include Synthetic Aperture Radar JERS-1, Terra-SAR, ALOS and PALSAR (Island et al., 2015). Among these technologies, the Lidar, which is a relatively new technology, has often used for effective forest monitoring, including biomass estimation. Lidar can model the vertical distribution of the canopy and ground surface, which will give full information about vegetation structure and it estimates the tree crown size, tree height, basal area and stem volume accurately (Vashum, 2012). However, the data set obtained from airborne Lidar and Radar is costly to use for regular monitoring and not always accessible.

Recently, the emerging of Unmanned Aerial Vehicles (UAVs') which are low-cost and lightweights are becoming operational. This platform is operated from the ground and provide a promising way for timely and cost-effective monitoring of environmental phenomena and natural resources at a very high spatial and temporal resolutions(Anderson & Gaston, 2013). UAV are platforms capable of carrying sensors for monitoring, and mapping of the environment and natural resources. It is used to detect fields of interest using different kinds of sensors and cameras. RGB sensor is assembled on UAV; however, other sensors like Sequoia and FireflEYE are installed for a particular application like agriculture, forest, and urban area because of their ability to capture data in different spectral bands. UAV- RGB platforms have low cost and flexible compared to other platforms. The RGB camera helps to produce high-quality point cloud, orthophoto and 3D images (Effiom et al., 2019).

1.2. Problem statement

The temperate forest ecosystem is rapidly changing due to high population growth, and related human activities like agricultural expansion, economic development, expansion of settlement, mining construction and infrastructural development (Potapov, 2009). Over 500 temperate forest tree species are threatened with extinction, as a result of over-exploitation. In some regions of Europe and Asia, the process of deforestation takes place for more than thousands of years but continued to be the main threat in many areas. Timber harvesting also going on in many parts of the world's temperate forests. As a result of these activities nowadays, temperate forests are fragmented, and the old forests are limited in extent (Newton & Featherstone, 2005). The loss and destruction of the forests caused the release of carbon into the atmosphere; which lead to the problem of climate change and global warming (Musselman & Fox, 1991).

Estimating the biomass and carbon stock is very critical to assess the sustainability and the productivity of the world's temperate forests. It furthermore helps to know the potential amount of carbon, which will be released to the atmosphere while the forests are burnt or cleared. Moreover, it helps to estimate the amount of stored carbon in the living biomass of the forest (Vashum, 2012). Forest biomass can be assessed using field measurements or in combination with remote sensing (RS) techniques. There are two main types of forest Above Ground Biomass (AGB) assessment methods. They are called destructive and non-destructive methods. The destructive method is the most accurate and direct method for assessing AGB/ carbon stock. This method is operated by harvesting and weighing different parts of the tree. This method mainly used to derive allometric equations for specific areas or the generic equation. The non-destructive method of AGB assessment is applied by measuring the diameter and height of the tree and convert to biomass using specific allometric equations (Island et al., 2015). The RS method is another way of estimating AGB/carbon stock of forests. These technique used to collect data from a distance without having direct contact with an object. It has the advantage to obtain data from large and inaccessible areas. Nowadays different kinds of data from remote sensing satellites are available in various scales, cost and accuracy. UAV data is widely used RS techniques due to its flexibility, cost and reasonable efficiency (Kumar & Mutanga, 2017).

Several studies have been conducted on forest AGB, and carbon stock using direct field measurement and RS techniques also by combining the field with RS derived data. But there are only limited studies available which concern with the accuracy of the digital terrain model (DTM), and its effect on the canopy height model (CHM) and then on the estimated AGB/ carbon stock. Ni et al. (2019) estimated the AGB/carbon stock using UAV leaf-on and leaf-off season images. The obtained result compared with the result obtained from Lidar data. The result of AGB/ carbon from UAV leaf-on and leaf-off season images showed a strong correlation with the Lidar derived result. Obeng-manu, (2019) also assessed the accuracy of DTM under different forest canopy density (open, medium, dense and riparian) by taking field measurements as a reference point. According to the result obtained, there is no significant difference observed on the result of CHM and AGB/carbon estimation for open, medium, and dense forest canopy; but substantial difference observed for the riparian forest.

Still, studies on assessing DTM accuracy under UAV RGB images of leaf-on and leaf-off conditions are rarely found. Moreover, studies on estimating AGB by combining different forest parameters from various data sources also limited in number. Height is a very critical tree parameter while estimating AGB. DTM which has better accuracy used to obtain good quality CHM plus helps to estimate better tree height, which has influence on AGB /carbon estimation. During the leaf-on season (summer) the trees has full canopy coverage and this makes the point cloud not to reach the ground due to its full canopy which has negative impact on the quality of the DTM. But, in February (leaf-off) season most of the deciduous trees in temperate forest shade their leaves, and the canopy of the forest becomes more open. This makes possible to see the ground through the canopy and more point clouds to hit the ground, which will help to generate relatively accurate DTM, which has a positive impact on CHM and consequently on AGB/carbon stock estimation. Regarding this, some research works reported that the images acquired in leaf-off condition have better performance to generate accurate DTM and CHM (Ni et al., 2019).

This research follows three different approaches to estimate AGB/carbon stock and comparatively developed a new method. The AGB was computed using DSM and DTM of the same season and also by combining the DSM and DTM from two different years and seasons. To estimate AGB for the leaf-off season, DSM is obtained from images of September 2019 (leaf-on) and the DTM from images of February 2020 (leaf-off) season. At the same time, the field measured DBH was combined with the Lidar height to compute Lidar AGB. The accuracy of UAV results derived from UAV images are validated with the Lidar derived results. Therefore, this study aims, to assess the seasonal effect of the canopy on the accuracy of obtaining DTM and consequently on accuracy assessment of CHM and AGB/carbon stock estimation using UAV RGB images of 2019 and 2020, in Haagse Bos Netherlands.

1.3. General Objectives

The general objective of the study is to assess the seasonal effect of the canopy on the accuracy of deriving DTM and consequently on the accuracy assessment of CHM and AGB/carbon stock estimation in the temperate forest of Haagse Bos, Enschede, The Netherlands.

1.3.2. Sub-objectives

1. Assess the accuracy of DTM obtained under the canopy of leaf-on and leaf-off seasons compared to Lidar DTM.
2. Compare the tree heights using CHM derived from UAV RGB images of leaf-on and leaf-off seasons.
3. Assess the relationship between the crown projection area (CPA) of the trees derived from UAV images and diameter at breast height (DBH) measured in the field.

4. Compare the AGB/carbon stock estimated from UAV RGB images of the leaf-on and leaf- off seasons and assess the effect of improved CHM on the accuracy of the resulted AGB/carbon stock.
5. Assess the accuracy of AGB estimated from UAV RGB images of leaf-on and leaf-off seasons compared to Lidar derived AGB.

1.3.3. Research Questions

1. What is the accuracy of DTM obtained from UAV RGB images of leaf-on and leaf-off seasons in comparison to DTM of Lidar data?
2. How accurate is the height of the trees derived from UAV RGB images of the leaf-off season compared with the leaf-on season?
3. What is the relationship between CPA derived from UAV images and DBH measured in the field?
4. What is the amount of estimated AGB/carbon stock for leaf-on and leaf-off seasons?
5. What is the effect of improved CHM on accuracy result of AGB/carbon stock?
6. How accurate is the AGB derived from UAV RGB images of leaf-on and leaf-off seasons compared to AGB derived from Lidar data?

1.4. Hypothesis

1. H0: There is no significant difference between trees height derived from CHM of leaf-on and leaf-off seasons.

   H1: There is a significant difference between trees height derived from CHM of leaf-on and leaf-off seasons.
2. H0: There is no significant relationship between CPA segmented from UAV RGB image and DBH measured in the field.

   H1: There is a significant relationship between CPA segmented from UAV RGB image and DBH measured in the field.
3. H0: There is no significant difference between AGB/carbon stock estimated from UAV RGB images of leaf-on and leaf-off seasons.

   H1: There is a significant difference between AGB/carbon stock estimated from UAV RGB images of leaf-on and leaf-off seasons.

1.5. Conceptual diagram

The system boundary for this research is Haagse Bos forest reserve Enschede, The Netherlands (Figure 1). Different forest types, foresters, researchers and the local communities are found within the system boundary. The forest gives various benefits to the local communities and for others by providing environmental and recreational services. Foresters are people who manage the forest by protecting from loss and damage, biodiversity, deforestation and degradation. Correspondingly, the researchers are people who conduct researches by measuring forest parameters. Outside the system boundary, the forest has put a positive influence on the climate by storing carbon from the environment, purifying and stabilizing the air. At the same time, the climate also affects the growth and productivity of the forest both positively and negatively.

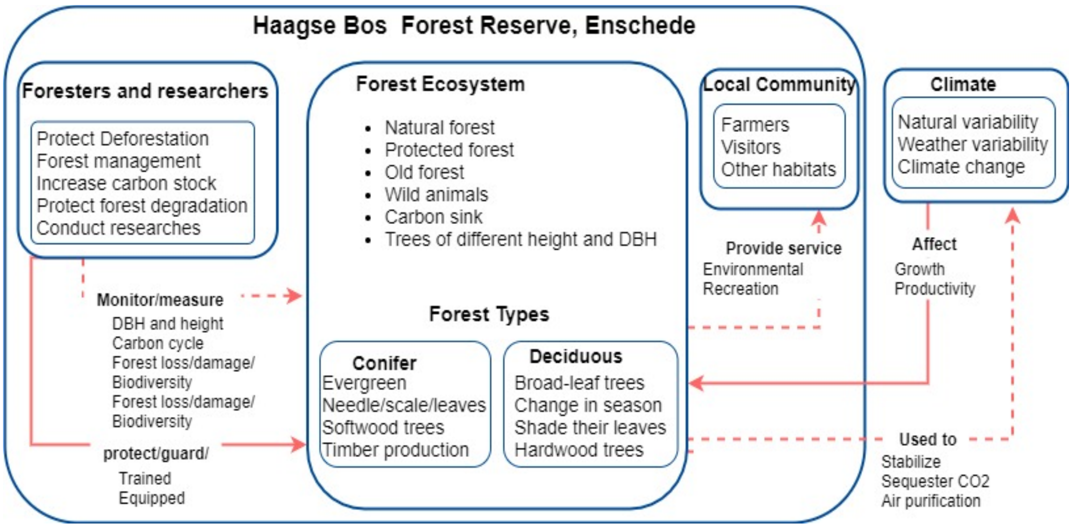

Figure 1: Conceptual diagram for interactions within the system.

2. CONCEPTS AND DEFINITIONS

2.1.Crown Projection Area (CPA) and Crown Diameter (CD)

Crown projection area (CPA) is the part of the forest floor which is covered by the vertical projection of tree crown (Jennings, 1999). CPA is a critical parameter to assess inter-tree competition and estimating biomass volume. Canopy cover is a vital variable required in estimating stand statistics from remotely sensed images (Ezenwenyi et al ., 2018). The canopy of the tree is the centre of physiological activity which indicates the potential photosynthetic capacity on a tree even though its measurement remains a challenge in forest inventory task (Chukwu et al., 2017).

Both crown diameter (CD) and crown projection area (CPA) can be measured in the field, but, the work is time-consuming, expensive and not accurate. The CPA is the total crown area of the tree whereas, the CD is calculated by measuring the width of the tree canopy. First, we measure width 1 (W1) and width 2 (W2) of the tree. W1 is the widest width of the crown, while W2 is the width perpendicular to W1. To calculate the average crown diameter, then add the two widths of the tree and divide it by two (Figure 2).

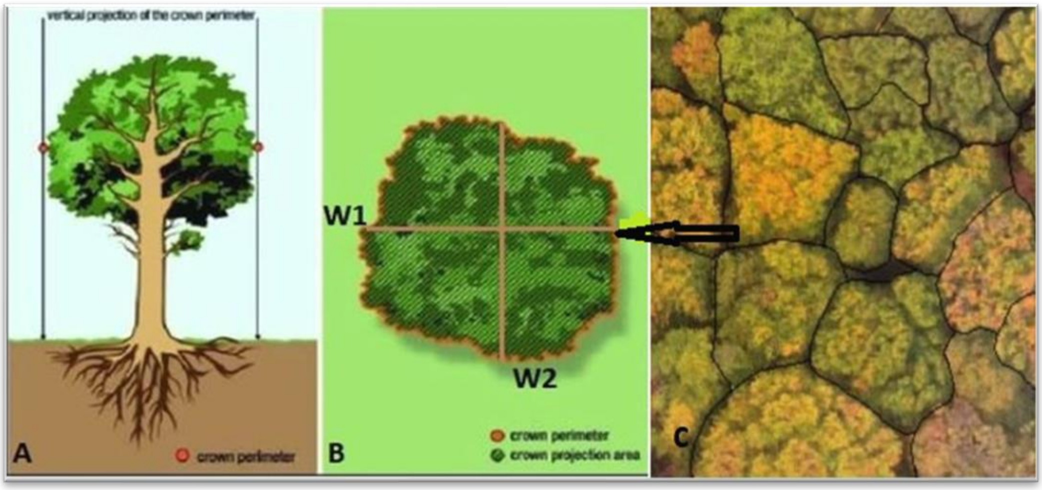

Figure 2: Crown projection area (CPA) and measuring crown diameter (CD).

Source: Modified from (Gschwantner et al., 2009).

CD= W1+W2/2

Equation 1: Calculating Crown diameter.

Where , W1 = width 1

W2= width 2

$CPA = \pi(CD^2)/4$

Equation 2: Calculating the crown projection area.

Where: CPA = Crown projection area (m2);

CD = Crown diameter (m);

π = Pi is constant

Besides the field measurement, the CPA can be generated by digitising and delineated the crown of individual trees from the generated orthophoto on ArcGIS software (Figure 2 C). Likewise, the CD can be derived from the CPA. This method is less time consuming and more accurate compared to the field measurement.

2.2. Temperate forest tree species

The temperate forests are mainly found in the mid-latitude areas. These forest types account about a quarter of the global forest. The tress in temperate forests is classified into two major tree categories of conifer and deciduous. The word conifer derives from the Latin word called " cone-bearing", which refers to the conical shell. Deciduous also came from the word "*decider"*, which has equivalent meaning with " fall off," to indicate the seasonal loss of leaves (Balliett, 2010).

Conifer trees are among the oldest and the largest trees in the world. They are called the softwood trees and are less dense compared to the deciduous tree species. Conifer trees include the needle- leaves species of pine, spruce and the Douglas fir and some scale leaves trees of cedar and juniper. The conifer trees keep their leaves throughout the year and remain green. The conifer tree species make up around one-third of the total forests in our world (Gorte, 2007). In the temperate forest ecosystem, the hardwood trees are called deciduous trees. Beech, birch, and alder are included under deciduous tree species (FAO, 1999). These trees are called the broad-leaf trees, and they comprise 65% of the global temperate forests. During the autumn season, the deciduous trees change the colour of their leaves and drop all annually (Dreiss & Volin, 2014). These trees bloom and begin their annual cycle during the spring season (Balliett, 2010).

Temperate forests regularly grow close to the farm and near to urban areas. These make them suitable to use them as recreational areas, non-forestry activities like hunting, fishing and as a place to collect mushrooms and fruits. However, they are used primarily as a leading source of industrial Roundwood trees. (FAO, 1999). Most of the temperate forests are utilized for commercial timber production, due to their moderate tree growth rate, species diversity, and suitable wood characteristics of most of the conifer trees (Gorte & Sheikh, 2010).

2.3. AGB/carbon stock estimation

Above-ground biomass (AGB) is an essential indicator for forest productivity, storage of carbon and sequestration (Calders et al., 2015). AGB is expressed as tonnes of carbon per ha and includes the steam, foliage and leaves biomass. The amount of carbon stored in the above-ground living biomass of trees is the largest pool contains the highest Percentage of biomass compared to the other pools, and it is also the most affected biomass by deforestation and forest degradation. Thus, estimating above-ground forest biomass is an essential step in measuring carbon stocks and fluxes from forests (Gibbs et al., 2007). Recently AGB estimation, mainly forest biomass, has received significant attention due to the increase in the problem of climate change and global warming. AGB estimates are becoming key for carbon inventories and worldwide agreements on carbon trading projects (Kumar & Mutanga, 2017). Forest carbon stock is estimated based on estimated biomass. There are no direct measurement methods for carbon stock. According to literature, around 50% of the dry biomass is carbon stock (Vashum, 2012). The carbon stock for above ground biomass computed using a conversion factor of 0.47 (depending on the species). The conversion factor is multiplied with the total biomass tone/ha, and the entire carbon stock is obtained (IPCC, 2006).

AGB estimation methods grouped into field measurement and the use of remote sensing techniques or a combination of the two (Wakawa, 2016). The field measurement classified into destructive and non-destructive techniques. The destructive approach is the most direct and accurate way to estimate AGB in the forest ecosystem. The way of estimation includes cutting of all trees in the particular area and dry and weigh the biomass in the steam, leaves and branches. The method is time and resources consuming, destructive, expensive, and feasible for large scale analysis (Kumar & Sharma, 2015). This method is very accurate for a particular location and impractical for country-level analyses. But this kind of technique used to develop biomass equations that may help to assess biomass on a larger-scale, e.g. using allometric equation (Gibbs et al., 2007).

The second method is also known as the non-destructive method. It can estimate the biomass of a tree without cutting down the tree. It is practical for those ecosystems with unique or protected tree species, where cutting of tree species is not operational or functional (Kumar & Sharma, 2015). Currently, different Remote sensing techniques, biomass expansion factor (BEF), regression models and biomass equations are used to estimate AGB by combining with field measurement techniques. RS method to estimate AGB is based on an indirect relationship with forest parameters, such as tree height and tree DBH. Accurate field measurement is needed to validate satellite-derived data (Wakawa, 2016).

2.4. Allometric equations

Biomass estimation equations are called allometric equations. Estimating biomass using the allometric equation is considered as a non- destructive method (Wakawa & State, 2016). It is developed and applied to forest inventory data to assess the biomass or volume of above-ground tree components based on DBH and tree height data. This equation is derived from measured values. The use of biomass equation is the most common and cost-effective method to assess the biomass of trees (Kebede & Soromessa, 2018). Various researchers have developed biomass equations for several types of forest and tree species. The equations are created by establishing a relationship between different tree parameters and developed for specific and a mixture of different species. It used to estimate the biomass for site-specific and large scale (Vashum, 2012).

The allometric equation has uncertainties which are related to the selection of variables and application. For instance, most of the general allometric equations does not consider the variation of the age and structure of the stand, soil type, climate, and generic properties. Some allometric equations are using DBH as the only predictor variable, but estimating the AGB without considering the tree height will cause variation in AGB. It is also affected by height and wood density and introduce error in carbon stock estimation and will give less accurate result (Chave et al., 2014).

2.5. Lidar Technology

Light detection and ranging (Lidar) is an active remote sensing technology, which can be used for the accurate measurement of distances. To measure the distance between the earth and the sensor, it uses the emitted pulses. Thousands of light pulses are collected into a "point cloud", which used to provide an accurate and 3D information about the surface of the earth and its characteristics (Calders et al., 2015). The emitted pulses from Lidar has multiple returns which, increase the ability to look at 3D information (Figure 3). The emitted pulses from the Lidar not only reflected and returned from the top of the canopy but pass through the canopy. Sometimes the Lidar pulse travels in between the tree leaves. The emitted light hits canopy of the forest and the ground surfaces and then reflected back to the sensor, having multiple returns from the ground and canopies (Gibbs et al ., 2007).

The Lidar system consists of a set of instruments like global positioning system (GPS), inertial navigational measurement unit (IMU) and a computer interface and the data storage (Starek, 2016).

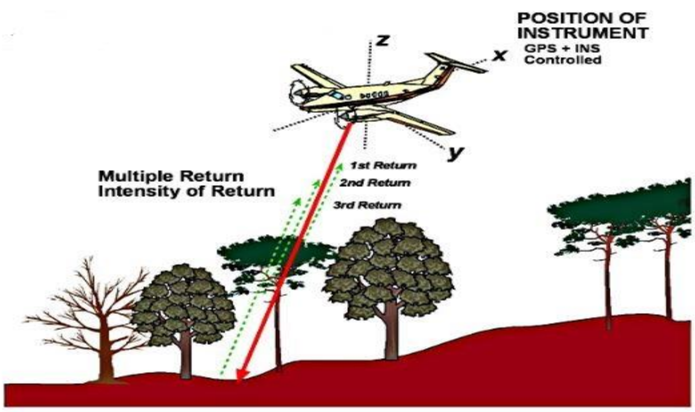

Figure 3: Lidar pulse returns while collecting different information about the surface.
Source:(Gatziolis et al., 2008);(Starek, 2016).

Lidar is a newly emerging remote sensing technology with promising capability for mapping, monitoring, and assessment of forest resources. Recently Lidar has been used to effectively assess and estimate the height and size of trees, volume, canopy closure, and forest biomass (Gatziolis & Andersen, 2008). It is also a popular source of data to generate a DTM very effectively over a large area in terms of precision and time (Polat & Uysal, 2018). The airborne topographic Lidar system is commonly used to generate digital elevation models over large areas. The airborne platform, together with scanning Lidar, is a very effective method to collect elevation data over areas of thousands of square miles (Peltonet al., 2013).

3. MATERIALS AND METHODS

3.1. Study area

This study is conducted in Haagse Bos, which is located at 7km distance from Enschede on North-Eastern direction. It is geographically situated between 476500m N to 477700m N and 261000m E to 262000 m E (Figure 4). The Haagse Bos consists of both the private and the natural monument forests. The trees planted on the private forest areas are mainly used for timber production. Previously the natural monument used to be a production forest, and all the trees were planted for the production purpose. Nowadays, due to the work of the natural monument, it is changing to a more natural forest. This forest area under the natural monument is managed and grown without any human intervention and not used for any production purposes. These forest areas primarily serve for environmental conservation and recreation purposes.

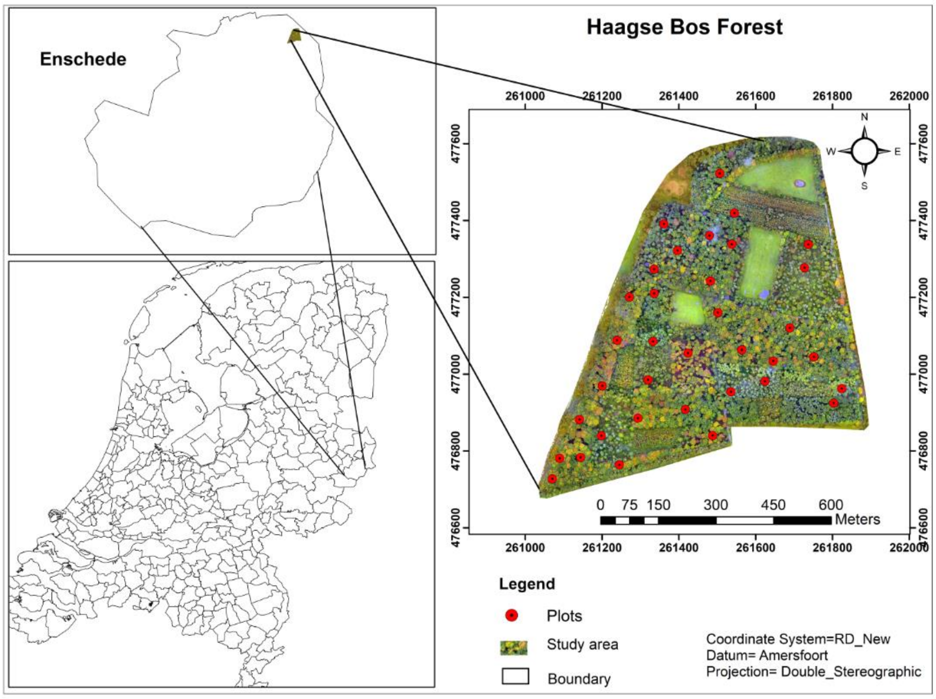

Figure 4: Map of the study area (Haagse Bos).

The study area covers 42 ha of forest land with eight different species of conifer and the broad-leaf trees. Most of the broadleaf or deciduous trees are grown in the area have almost the same age structure. The conifer tree species are the Scots pine (*Pinus sylvestris*), Norway spruce (*Picea abies*), and the Douglas fir (*Pseudotsuga menziesii)* trees. The broadleaves are European beech (*Fagus sylvatica*), European larch (*Larix decidua*), Oak (*Quercus robur*.), European white birch *(Betula pendula) and* Alder *(Alnus glutinosa)*. Broad-leaf trees are found dominantly in the natural monument forest, and only a few numbers of conifer trees are available. From the broad-leaf tree species European beech (*Fagus sylvatica*) is the leading tree species in the area and followed by Oak (*Quercus robur*.) species.

3.2. Materials

3.2.1. Data Source

Both primary and secondary data are used as input for this study. The primary data are obtained from Lidar and UAV images, field survey and GPS measurement, whereas the secondary data were from existing data sources (Table 1).

Table 1: Lidar, UAV and field data types and sources.

No	Data	Source
1	UAV images of leaf-on and leaf-off seasons	UAV RGB Sensor (DJI Phantom 4)
2	Sample plots and coordinates	Field survey, GPS
3	DBH, species type, distance, bearing and coordinates	Field survey and measurements
4	Ground control points (GCPs) and coordinate of plot center	Global navigation satellite system real-time kinematic (GNSS RTK)
5	Lidar DTM and DSM	Actueel Hoogtebestand Netherlands (AHN)

3.2.2. Equipment

Different types of equipment and instruments were used in the field to measure important forest parameters (Table 2). These parameters play an important role in AGB/carbon stock estimation.

Table 2: List of field equipment and their use.

No	Equipment	Purpose
1	GPS receiver	Navigation and coordinates
2	Diameter Tape	Measure DBH
3	Suunto Clinometer	Measure angle and bearing
4	Digital camera	To capture photos
5	Datasheets	Record measured parameters
6	DJI Phantom 4	Capture UAV images
7	GNSS RTK	Collect GCPs and location of plot center
8	GCP markers	Mark GCPs
9	Leica Disto	Measure the distance of trees from plot center

3.2.3. Software

The following list of software (Table 3) used to process, analyse and interpret the collected data from the field measurement, UAV and Lidar images.

Table 3: List of software and tools used for data processing.

No	Software	Purpose
1	Pix4D Capture	UAV flight planning
2	Pix4D Ctrl+DJI	UAV drone imagery captured
3	Pix4D Mapper	UAV image processing
4	LAS Tools package in ArcGIS	DSM, DTM and CHM processing data
5	yEd	Flowchart drawing
6	ArcGIS 10.7.1	To generate CHM, Crown delineation, and producing maps
7	ERDAS IMAGINE	Data pre-processing
8	Microsoft Excel	Data analysis
9	Microsoft Word	Writing report
10	Mendeley Desktop	Citation, referencing and organize documents
11	Microsoft PowerPoint	PowerPoint presentation

3.3. Workflow

The diagram under (Figure 5) shows the overall workflow of the method, which is aimed to answer the research question. The workflow has three main sections. The first part describes the steps for field data processing. Biometric data collected includes only DBH. The field measured DBH used to combine with Lidar tree heights to estimate the Lidar AGB. On the second step, the Lidar obtained DTM was used as a reference to assess the accuracy of UAV derived DTM of leaf-on and leaf-off seasons. The Lidar CHM was generated by subtracting Lidar DTM from Lidar DSM. The tree heights extracted from Lidar CHM combined with field measured DBH used to estimate Lidar AGB and AGC.

The third part of the workflow shows UAV data processing which is based on the data from UAV leaf-on and leaf-off seasons. The first UAV images are captured on 12th of September 2019 which represent the leaf-on season and the second UAV images are captured on 14th of February 2020 on the leaf-off season. This part show steps for generating the point cloud, orthophoto, DSM, DTM, CHM, extraction of tree heights, CPA and DBH. The CHM from UAV images were generated in two ways: first generated from DSM and DTM of the same season (leaf-on). The second CHM was generated by combining the DSM from the leaf-on and DTM from the leaf-off season images. The tree heights extracted from CHM of leaf-on and leaf-off seasons are compared to see how much they fit and deviate from each other. Finally, the extracted tree heights combined with predicted DBH to compute AGB/AGC of UAV leaf-on and leaf-off season.

On the last step, UAV derived AGB/AGC was compared with each other, and the error was assessed. The accuracy of UAV derived AGB/AGC was assessed compared to Lidar AGB/AGC.

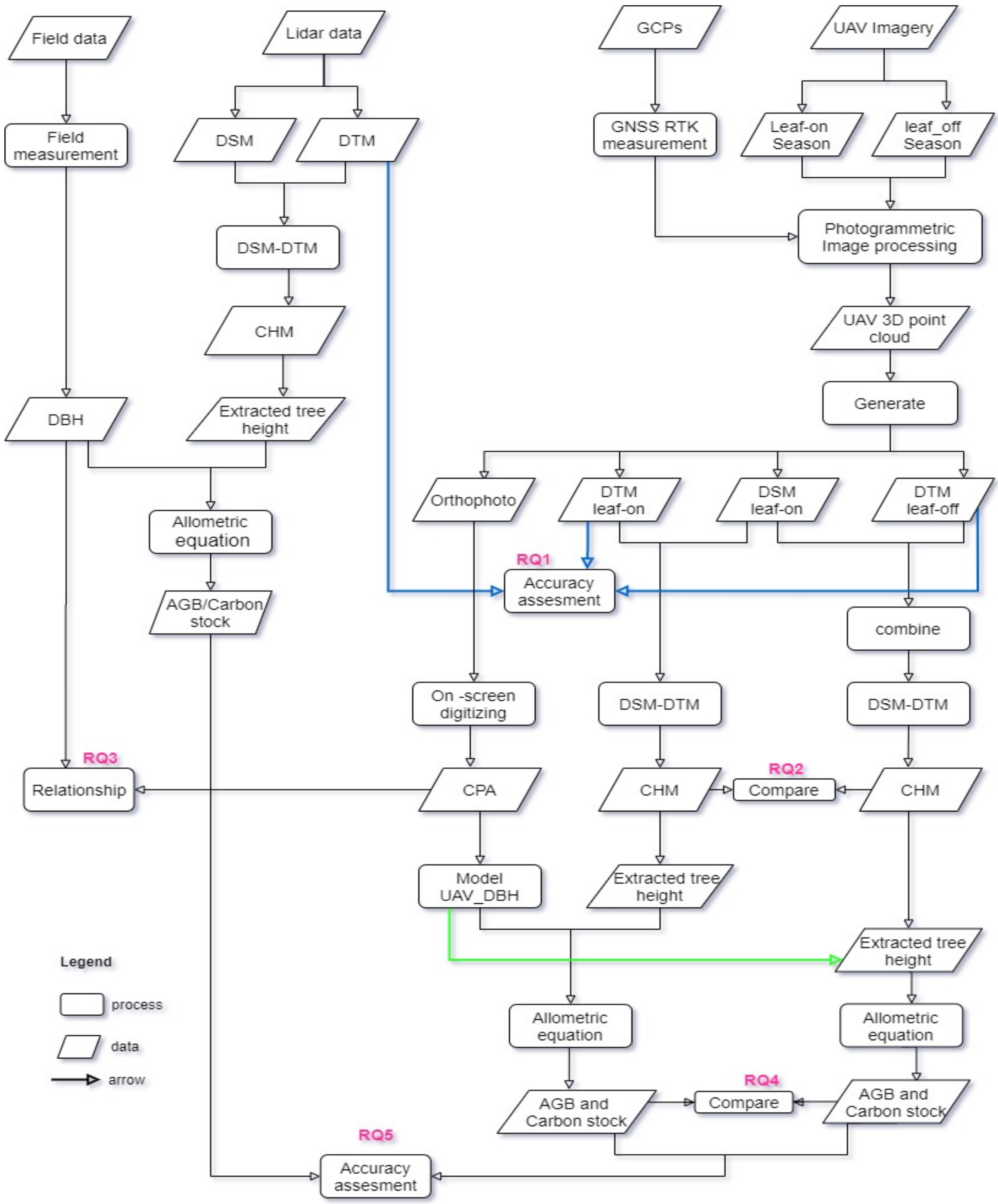

Figure 5: Methodological workflow of the study.

3.4. Fieldwork Planning

3.4.1. Sample plot design and size

Purposive sampling method was used due to time, weather and working force constraints. On the other way the availability of the same kinds of species within one or consecutive plots makes me choose a better area which has more species diversity, and to avoid plots which have many numbers of dead trees. It also helps me to mix both old and young plantation in my sampling.

Variety of sampling plot sizes and shapes are used to describe forest structure, biomass and ecosystem carbon pools. No single plot shape and size is optimal. But compared to others, the circular plots are relatively simple and easy to establish and efficient to measure (Kauffman & Donato, 2012). Circular plot area is 500m² or 0.05ha, which is a reasonable plot size for our study. The plot is placed on the ground by using a radius of 12.62 meters on flat terrain. A total of 35 circular plots were distributed within the study area (Figure 6). The X and Y coordinate of each plot center is measured with GNSS RTK to protect the shifting of the points. Once the center is identified, the radius was measured, and consequently, the border of the plot was defined. Thus all trees inside the plot were marked, identify and measured.

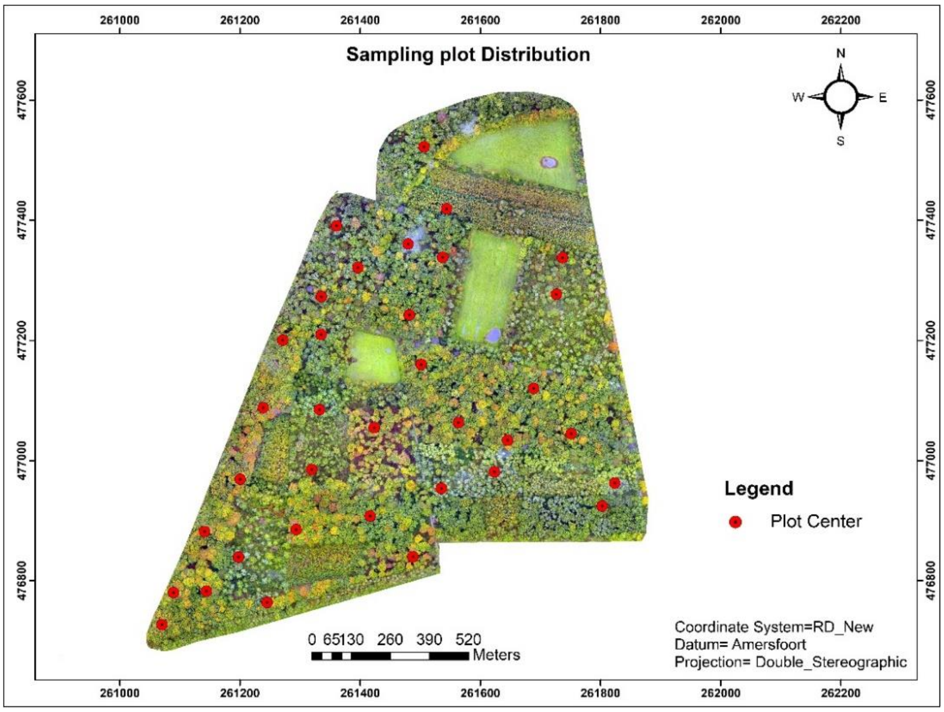

Figure 6: Distribution of sampling plots over the study area (Haagse Bos).

3.4.2. UAV flight planning and image acquisition

Two different season UAV RGB images was acquired by DJI Phantom 4. The same flight planning was used in both flights but different seasons. These flights are made to assess the seasonal effect of the canopy on the accuracy of DTM, CHM and consequently on the estimated AGB. The flight was made after placing and distributing the required amount of GCPs within the flight zone. The flight was done with a height of 120 meters above the actual terrain to achieve very high spatial resolution data with 4.61 and 4.75cm of ground sampling distance (GSD) for leaf-on and leaf-off seasons images respectively. The flights are made in a double grid flight fashion to produce better quality images, and slow flight speed was used to minimise blurring effect on the images. The image overlap which used in this flight was 90% and 80% for both front and side overlap respectively. All detail of planning information is given in Figure 7 and Table 4. An example of images collected during leaf-on and leaf-off seasons were shown in Figure 8.

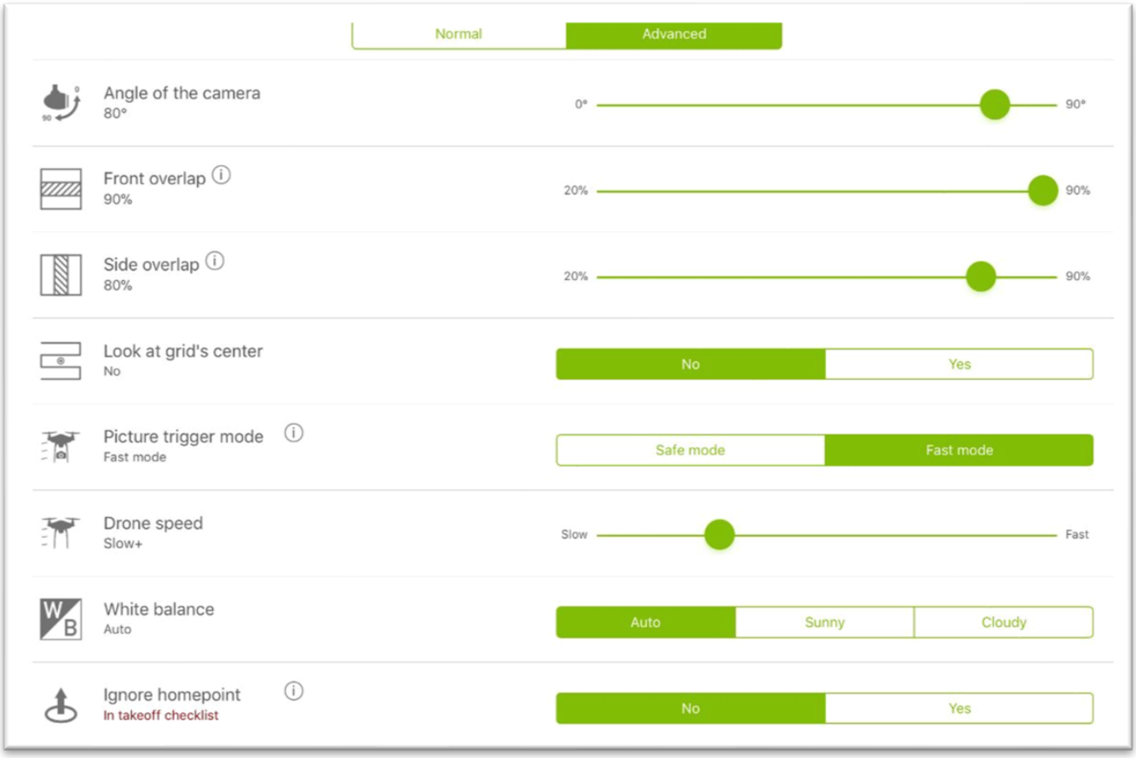

Figure 7: UAV flight planning used to capture images of the study area.

Table 4: UAV flight planning parameters for imaging in both seasons.

No	Parameters	Detail
1	Sensor	Phantom 4 DJI Drone (RGB)
2	Focal length	4mm
3	GSD	4.61 cm (leaf-on) and 4.75 cm (leaf-off)
4	Flight height	120 m
5	Front and side overlap	90 %, and 80 %
6	Flight pattern	Double grid
7	Flight line	Polygon double grid type (North-south direction)
8	Flight speed	Slow
9	Application used	Pix4Dcapture & Ctrl+DJI
10	GCPs	7 (leaf-on) and 8 (leaf-off)
11	Image Coordinate System	WGS 84 (EGM 96 Geoid)
12	GCP Coordinate System	Amersfoort / RD New (EGM 96 Geoid)
13	Camera speed	5.1623 m/s

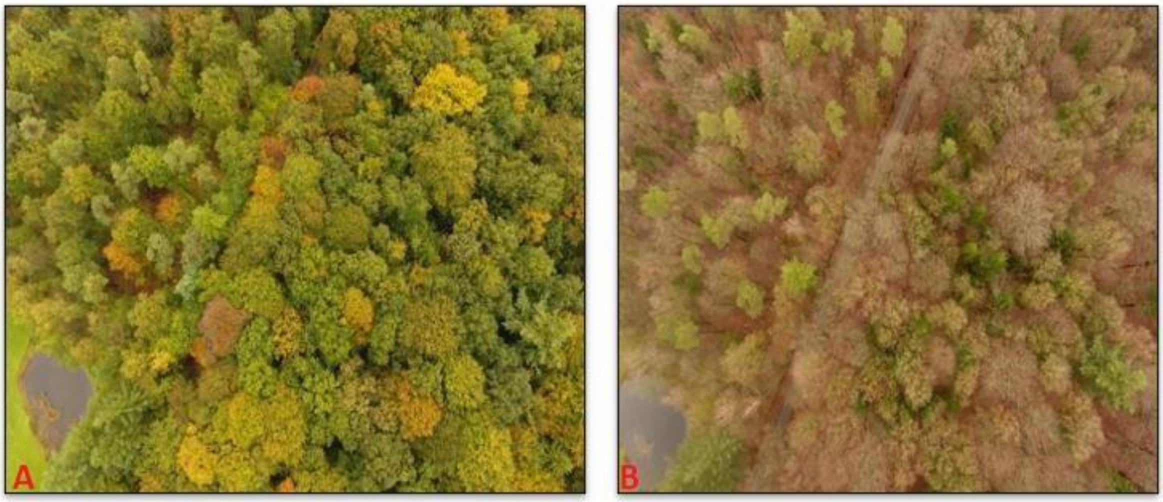

Figure 8: Images of the same area captured during leaf-on and leaf-off seasons.

As clearly shown on Figure 8, the image 'A' was captured during the leaf-on season and the leaves for both conifer and broad-leave trees was green. On image 'B' (leaf-off) season all the broad-leaf trees has shaded their leaves, and coniferous are still green.

3.4.3. Ground control points

The Ground Control Points (GCPs) were allocated to support spatial referencing of the 3D model generated from the images. The GCP points were pre-placed and well distributed on the surveyed area in a position that can be seen by the UAV. In addition to the GCP marks, the permanent points (E.g. pole, stone and corner points) were used (Appendix 2). The location of the GCPs and the permanent points are measured with high accuracy using differential GPS. Some of the GCPs were used as checkpoints (CP) for quality assessment purpose. For leaf-on season a total of 7 GCP were collected, from these 3 points used as a GCP, and the remaining four assigned as a checkpoint during image processing. Similarly, for the leaf-off season from the total of 8 GCPs collected, four used as a GCPs and the remained four as a checkpoint (Figure 9).

Figure 9: Distribution of GCPs over the study area while capturing the images.

3.5. Biometric data collection

The process of field data collection was started after processing the UAV data of the two seasons. The orthophoto generated from the UAV images of the leaf-on season was used to locate the proposed sample plots. The shapefile for all samples was prepared on ArcGIS and uploaded on google map pro in order to quickly identify the plot's location. On the beginning, a total of 80 sample plots were located on the orthophoto. I made a direct observation in the selected plots with the help of the google earth pro. But some plots are ignored due to absence of an expected number of trees within the plots due to logging, presence of more dead trees and young plantation which is less than 10cm DBH and presence of the same number of tree species between consecutive plots. For these reasons from the proposed 80 plots, only 35 plots were selected.

The field data were acquired in the period between 1-14 March 2020. The field measured parameters included DBH, tree species, GPS points, distance from plot center to each tree, bearing and some field photos. The measurement is made for all trees situated within 12.62 radii (Figure 10).

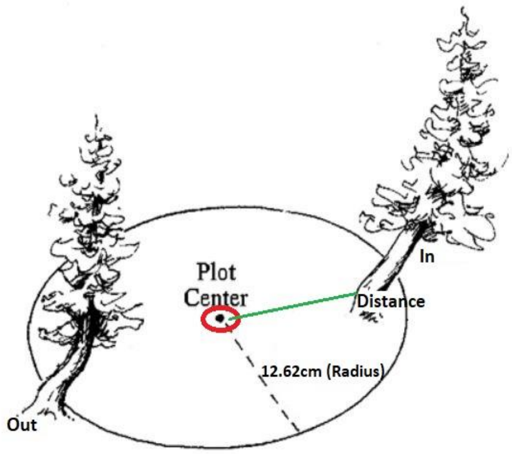

Figure 10: Figure showing the structure of the plot.
Source: Modified from https://developer.fulcrumapp.com/

Diameter at breast height (DBH) was measured at 1.3 m height above ground for all types of trees. Diameter tape 5m was used to measure the DBH. Only trees which are 10cm DBH and above were measured (Figure 11B). Leica Disto was used to measure the distance of the trees from the plot center. The bearing measurement was made using Suunto clinometer. The global navigation satellite system (GNSS) RTK were used to measure and record the coordinate of the plot center and the elevation of the area (Figure 11A). The collected data were recorded manually in tale sheets and later used as an input for analysis in Microsoft Excel. The measured GPS points were automatically stored using GNSS RTK and subsequently downloaded for analysis. The 'x' and 'y' coordinates of each tree were computed using distance and bearing measured in the field by taking coordinate of the plot center as a reference.

Figure 11: Plot center (A) and DBH measurement (B) in the field.

3.6. Data Processing

3.6.1. Biometric data processing

The field data includes the 'x' and 'y' coordinates of the plot center, tree species, DBH, distance and bearing from the plot center. These parameters were measured manually in the field and recorded in Microsoft Excel (Table 5). The recorded data were used as an input for analysis on excel, and ArcGIS. For this study, a total of 544 trees were measured from 35 plots.

Table 5: Field measured tree parameters registered on excel.

Plot no.	1				
X	261070.389				
Y	476727.031				
Elevation	52.021				
Tree no.	Species	DBH (cm)	Height (m)	Distance from PC (m)	Bearing from PC (m)
1	Oak	34	32	5.5	23
2	Larch	51	33	7.1	60
3	Beech	11	6	9.2	66
4	Beech	63	31	12	96
5	Larch	15	33	3.5	115
6	Beech	38	11	9.1	125
7	Oak	44	31	11	134
8	Larch	44	33	8.3	150
9	Larch	44	35	9.8	171
10	Beech	32	28	10.5	189
11	Beech	45	30	8.5	197
12	Beech	39	34	5.4	215
13	Larch	27	20	10.4	244
14	Larch	40	34	3.5	235
15	Oak	29	18	11.4	256
16	Beech	45	32	9.9	268
17	Beech	30	32	7.6	298
18	Larch	48	31	10.5	311
19	Larch	44	37	7.2	335
20	Oak	33	30	6.4	350

Plot1 | Plot2 | Plot3 | Plot4 | Plot5 | Plot6 | Plot7 | Plot8 | Plot9

The ‘x’ and ‘y’ coordinates of individual trees in the plot were calculated on a separate excel sheet using the coordinates of the plot center, distance and bearing measured in the field (Appendix 4). The bearing of each tree was measured from North to East in a clockwise direction. For example, to find the coordinate of the point “B” from figure 12, first, we need to calculate the departure (line parallel to the East line-BC) and the latitude (line parallel to the North line -BD).

Equation 3: Calculating departure BC= Lx SIN (θ)

Equation 4: Calculating latitude BD= Lx COS (θ)

So, Easting of point “B” = Easing of point A +departure. Similarly, to find Northing of point “B”= Northing of point A+ Latitude (Figure 12).

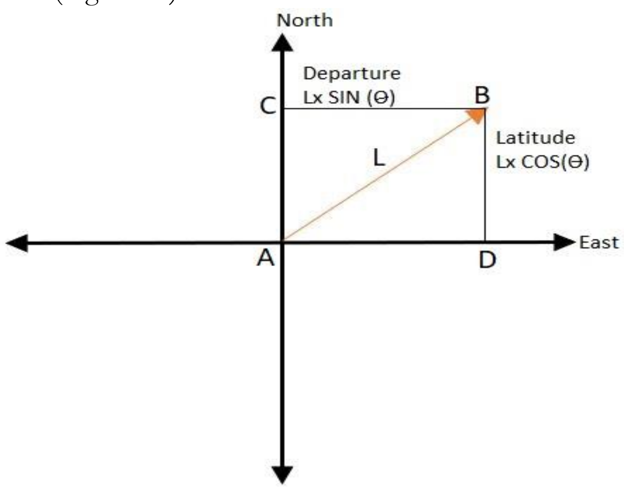

Figure 12: Calculating coordinates of unknown points.

3.7. UAV image processing

3.7.1. Processing Steps

Point clouds are a 3D sequence of points from space. 3D point clouds are automatically generated from Pix4D Mapper using Structure from Motion (SfM) technique (Iizuka et al., 2018). SfM is a photogrammetric method of constructing a three dimensional (3D) model based on multiple and overlapping two-dimensional images (Polat & Uysal, 2017).

Image processing workflow on Pix4D included three main stages (Figure 13): initial processing, point cloud densification and classification and DSM, DTM and Orthomosaic generation. The initial processing stage consists of key point extraction and matching, camera optimization and geolocation of the GCP. In this step, the software runs Automatic Aerial Triangulation (AAT) and the Bundle Block Adjustment (BBA). The initial processing is the foremost step because it serves as the base for the second and third stages. In the second processing stage, the users are allowed to define parameters for point cloud densification and classification. In the last processing stage, users can change the processing options and the desired outputs. It includes four main parts:-

- Resolution -define the spatial resolution,
- DSM filtering - set parameters to filter and smooth the point cloud used to obtain DSM,
- Raster DSM - select output format for raster DSM, and
- Orthomosaic- choose the output format for orthophoto.

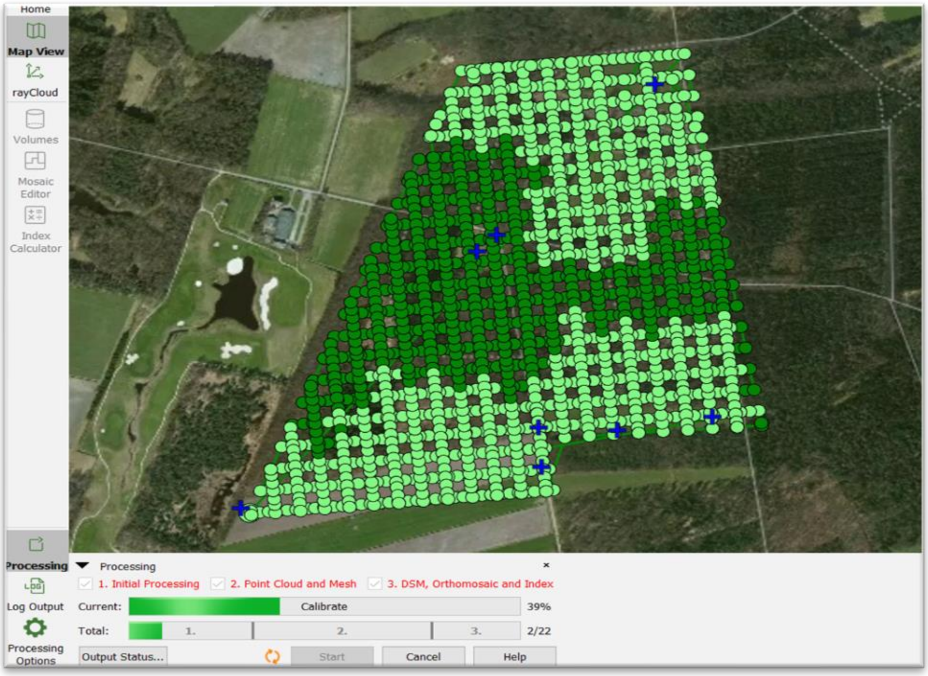

Figure 13: The three main Pix4D image processing stages.

3.7.2. DSM, DTM and Orthomosaic Generation

The digital surface model, digital terrain model, and orthophoto are generated from the 3D point cloud. Digital Surface Model (DSM) is a 2D map. Whereas, Digital Terrain Model (DTM) is described as a 3D representation of terrain surface consisting of X, Y and Z coordinates in digital form. The DSM includes the natural and human-made features found on the earth surface, while the DTM shows the ground surface of the earth (Zietara, 2017).

The DSM, DTM and orthophoto from two different datasets (leaf-on and leaf-off season) images were processed independently. At the initial processing stage, standard calibration and all prior internal parameters optimization methods were used. On the second stage, half image scale with the multiscale processing options was used. The optimal point density and number of image matches are set to three. Once the image processing completed, the software produced a quality report (Appendix 5 and 6).

From the report, the mean GCP RMS error was 0 and 0.001 m for leaf-on and leaf-off seasons respectively. At the same time, 61138701 and 74539481 3D densified points were produced for the leaf-on leaf-off season. The generated average density of points were 30.3 and 33.05 per/m^2 for leaf-on and leaf-off season. This supplied adequate quality of point cloud data for further processing (DSM, DTM and Orthomosaic).

The DSM and ortho mosaic shown was only obtained from UAV leaf-on season image. The orthophoto was mainly used for digitizing the tree crown with the help of the tree shapefile measured in the field. The Digital Surface Model (DSM) has value ranges from 43m (low) to 90m (high) (Figure 14).

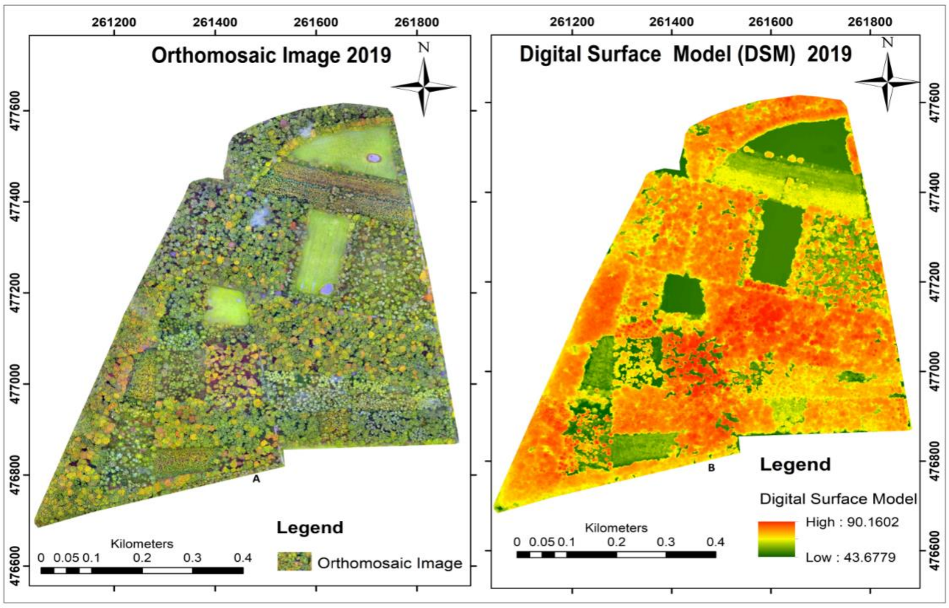

Figure 14: Orthomosaic image (A) Digital Surface Model (B) from the leaf-on season.

The digital terrain models were generated from both UAV leaf-on and leaf-off season images. The images captured on the leaf-off season was used only to obtain the digital terrain model (DTM). The DTM values generated from leaf-off season images range from 41 to 81 m, which is a bit higher than the DTM of the leaf-on season image, which ranges 43 to76 m (Figure 15).

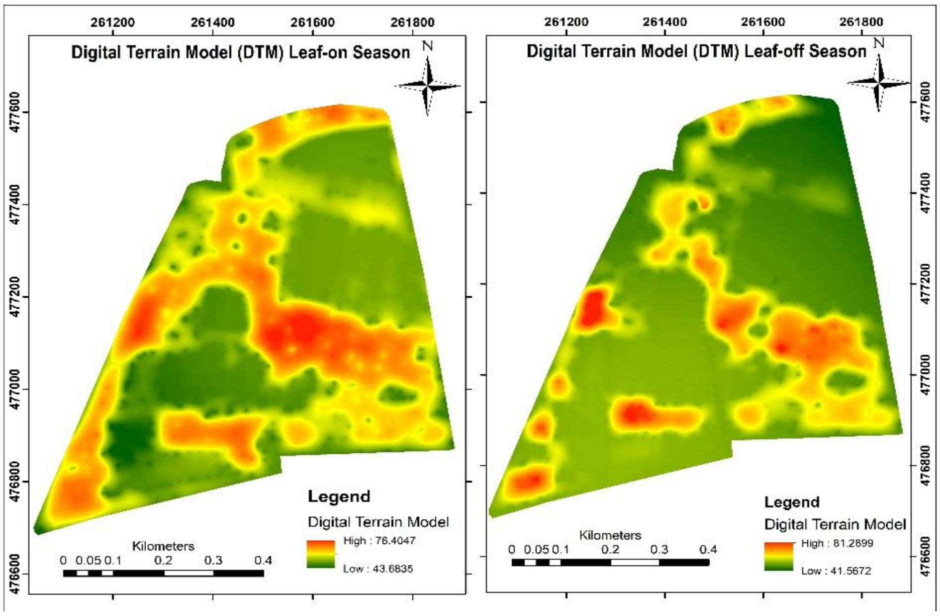

Figure 15: Digital Terrain Model (DTM) of 2019(leaf-on) and 2020 (leaf-off) seasons.

3.7.3. Canopy Height Model (CHM) Generation

The canopy height model (CHM) is the difference between Digital Surface Model (DSM) and Digital Terrain Model (DTM). CHM is created by subtracting the digital terrain modek (DTM) from the digital surface model (DSM). The process of subtracting the DTM from the DSM is done in ArcGIS software using the raster calculator tool. The canopy height model shows the real height of trees, buildings on the ground and the height of objects are determined by using the CHM (Polat & Uysal, 2017).

The CHM for the leaf-on season is generated by subtracting the DSM and DTM of the leaf-on season. Wheres as CHM for the leaf-off season was created by combining the DSM and DTM of different season images. The DSM is obtained from the image of the leaf-on season and DTM from the leaf-off season (Figure 16).

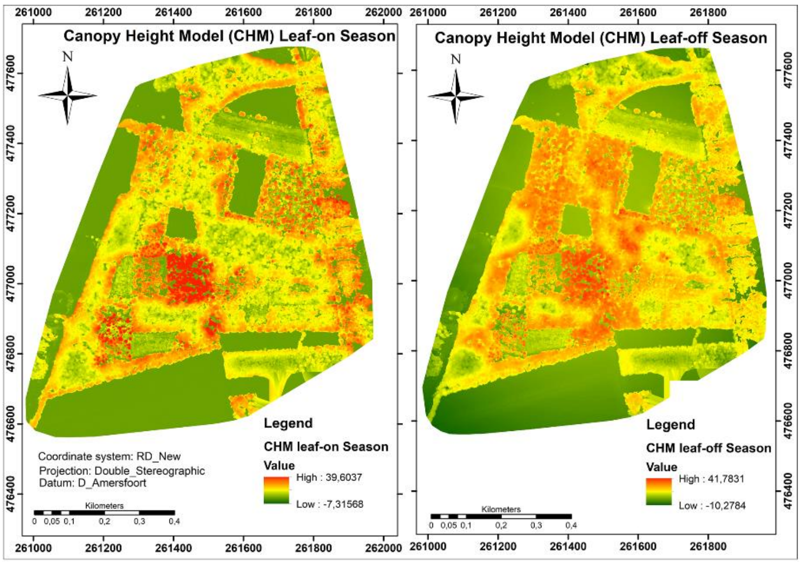

Figure 16: Canopy Height Model (CHM) for leaf-on and leaf-off season.

3.7.4. On-screen digitization

Manual on-screen digitization is a technique used to delineate features on screen. The canopy projection area (CPA) of each tree were digitized using the orthophoto generated from UAV leaf-on season image. The location of each tree in the plot was identified with their coordinates and digitized separately on ArcGIS software. Individual trees in the plot are digitized by overlaying the tree shapefile with the orthophoto. The trees within the plot area were digitized. Tree ID was given in order to make the matching easier. As shown in Figure 17, the red point is the center of the plot; the yellow points indicate the trees within the plot, and the numbers on tree crowns are IDs given for each tree after digitization. The ID P8_T1 stands for plot eight tree one. The area of the CPA was calculated and used to model the DBH and to estimate the UAV tree height. The tree height derived from CHM of UAV leaf-on and leaf-off seasons images together with predicted DBH used to estimate the UAV based AGB/carbon stock.

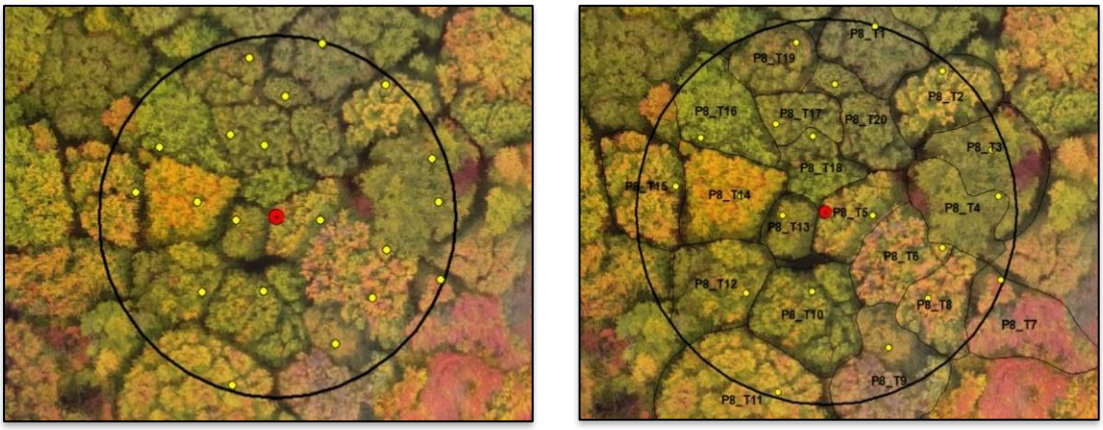

Figure 17: The location of the trees within the plot and on-screen digitization.

3.8. Lidar data processing

The Lidar DTM and DSM were obtained from the "Actueel Hoogtebestand Netherland (AHN)" or the Current Elevation of Netherlands (www.ahn.nl) in raster format. The CHM was generated in ArcMap by subtracting the DTM from the DSM. The process of resampling and masking the Lidar data also made in ArcMap. The generated CHM was used to extract the tree heights by overlying with digitized crown shapefile and coordinate of trees.

3.9. Data Analysis

3.9.1. Accuracy assessment

The DTM accuracy assessment was made by comparing the UAV DTM with the Lidar DTM values. First, the cell size of the UAV leaf-on, leaf-off and Lidar DTM were matched. The UAV leaf-on and leaf-off seasons have a cell size of (GSD) of 4.61 and 4.75cm, respectively. Whereas, the Lidar DTM has a cell size of 0.5m (50cm). To make a better comparison and extracted values from similar areas, the UAV DTM was resampled to the Lidar DTM cell size. The process of changing the cell size (resampling) was made in ArcGIS software, and random points were given. The tool from ArcMap used to distribute the random points, and the points were used to extract the elevation values from each DTM. The accuracy assessment was made based on the values obtained. The elevation values from the UAV DTM of leaf-on and the leaf-off season was compared with Lidar obtained values. In this case, the Lidar DTM was used as a reference point to validate UAV DTM. The comparison was made using 100 random points to extract elevation values from both UAV and Lidar DTM. The points were randomly distributed all over the study area.

Above-ground biomass (AGB) was estimated from Lidar and UAV datasets. The AGB from the UAV datasets was estimated using height extracted from UAV images of leaf-on and leaf-off seasons and predicted DBH. Tree heights were extracted from the Lidar CHM and combined with the field measured DBH to estimate Lidar AGB. The obtained results were compared, and AGB from the Lidar data was used as a reference to assess the accuracy of the UAV derived AGB.

3.9.2. Comparing UAV tree height

The CHM obtained from UAV leaf-on and leaf-off seasons are used to extracted individual tree heights. The process of extracting the tree height was made in ArcGIS software using zonal statistics. The tree heights are generated from the CHM using the crown polygon digitized from the orthophoto and the tree height raster. Individual tree height values will be obtained by overlaying the tree and the crown shapefile with the raster CHM. The extracted tree heights were compared using a scatter plot. The R^2 and RMSE were used to show how they fit or deviate from each other. The error was estimated in order to identify how much error was propagated to carbon estimation.

3.9.3. The relationship between CPA and DBH

The CPA digitized from UAV imagery in combination with the field measured DBH used to predict (model) the UAV DBH. The relationship between the UAV derived CPA and Field measured DBH tested using different regression models. Linear, quadratic, logistic and power models were used to test DBH-CPA relations. The one which showed better performance and accuracy (higher R^2 and lower RMSE error) was used to predict the UAV based DBH. From a total of 544 trees located in 35 plots, some of the trees were selected with their field measured DBH for the purpose of model development and validation.

3.9.4. Statistical Analysis

Various statistical analysis was carried out to achieve the objectives of the study. The regression analysis was used to assess the relationship between the dependent and independent variables. R^2 used to measure how the data are fit with each other. It is shown using the values zero to one. In this case, it was used to show the relationship between field-measured DBH and CPA, the tree height obtained from the UAV CHM of leaf-on and leaf-off seasons and estimated AGB from Lidar and UAV datasets. The mean and the variance were compared using the t-test and F-test. RMSE was used to show the error (deviation) of the analysed datasets. The equations used for RMSE and % RMSE are shown below.

$$RMSE = \sqrt{\sum_{i=1}^{n} \frac{(\hat{y}_i - y_i)^2}{n}}$$

Equation 5: Equation for RMSE calculation.

Where,

RMSE= Root Mean Square Error

ŷ1,ŷ2,…………………………,ŷn are predicted values

y1,y2,………………………..., yn are observed(actual) values

n……………………………...is the number of observations

RMSE is usually written as a percentage error (multiply RSME by 100%).

$$\%RMSE = RMSE * n * 100 / \sum X_{obs}$$

Equation 6: Equation for RMSE% calculation.

Where,

%RMSE = Percentage of Root Mean Square Error

n = Number of sample size

Xobs = Observed value

3.9.5. Species-specific allometric equations

Eight different sites and species-specific allometric equations were proposed for this study. The use of the general allometric equation to estimate the biomass of diverse forest may cause uncertainty due to environmental variation. Therefore, only the equation developed for Dutch forest is used to accurately quantify the biomass (Daba & Soromessa, 2019). All the equations are obtained from (Zianis et al., 2005) (Table 6).

Table 6: Different allometric equations selected to estimate the AGB per species.

	Species	Allometric Equations	R^2	Country
1	Oak(*Quercus robur.*)	$AGB = D^{2.00333}.H^{0.85925}.exp(-2.86353)$	0.995	Netherlands
2	European Larch (*Larix decidua*)	$AGB = D^{1.86670}. H^{1.08118}.exp(-3.0488)$	0.996	Netherlands
3	Scot pine (*Pinus sylvestris*)	$AGB = D^{1.82075}.H^{1.07427}.exp(-2.8885)$	0.994	Netherlands
4	Douglas fir (*Pseudotsuga menziesii)*	$AGB=D^{1.90053}.H^{.80726}.exp(-2.43151)$	0.993	Netherlands
5	Norway spruce (*Picea abies*)	$AGB = 0.04143.D^{1.6704}.H^{1.3337}$	0.995	Netherlands
6	European white Birch*(Betula pendula)*	$AGB = D^{1.89060}.H^{.26595}.exp(-1.07055)$	0.999	Netherlands
7	European Beech(*Fagus sylvatica*)	$AGB = 0.049 .D^{1.78189}.H^{1.08345}$	0.999	Netherlands
8	Alder*(Alnus glutinosa)*	$AGB=D^{1.85749}.H^{0.88675}.exp(-2.5222)$	0.991	Netherlands

Equation 7: species allometric equations.

Where,

AGB=Above ground biomass kg/tree, D= Diameter at breast height (cm), H= Tree height (m)

The conversion factor (CF) will be used to convert the above-ground biomass into carbon stock. This will be done by multiplying by CF =0.47 (IPCC, 2006) (Equation 8).

C =AGB*CF

Where,

C=Carbon stock (mg), CF=conversion factor

Equation 8: Carbon conversion factor.

3.9.6. Error assessment

There are different potential sources of error which propagate to biomass and carbon estimation. The error can be propagated from DBH, tree height, and canopy density measurements. These errors are mainly propagated to the AGB/AGC through the allometric equation. The other sources of error related to the; improper selection of the allometric equations and methodological sources. Errors caused related to methodology include the incorrect estimation of the plot area, missed trees, measuring twice, counting dead trees as alive, and CPA digitization (Chave et al., 2004). In this study, the error was propagated from the difference in canopy density from the two seasons. The error in this case only related to the height difference in the two UAV datasets. All other errors are the same for both cases.

4. RESULT

4.1. Descriptive Statistics of the biometric data

The descriptive statistics of the biometric data includes DBH measured in the field as well as different species observed and recorded from the field. It helps to understand the type and the nature of the data collected.

4.1.1.Types and number of tree species

A total of 35 sample plots with 500m^2 was used for this study. From these plots, 544 trees with eight different species were identified. The identified species include Alder (3%), Beech (31%), Birch (11%), Douglass fir (5%), Larch (4%), Oak (28%), Pine (6%) and Spruce (12%). As indicated in Figure 18, deciduous tree species are the most abundant compared to the conifer trees. Among the deciduous trees, Beech and Oak take the lion share, whereas Alder is the least abundant tree species in the study area.

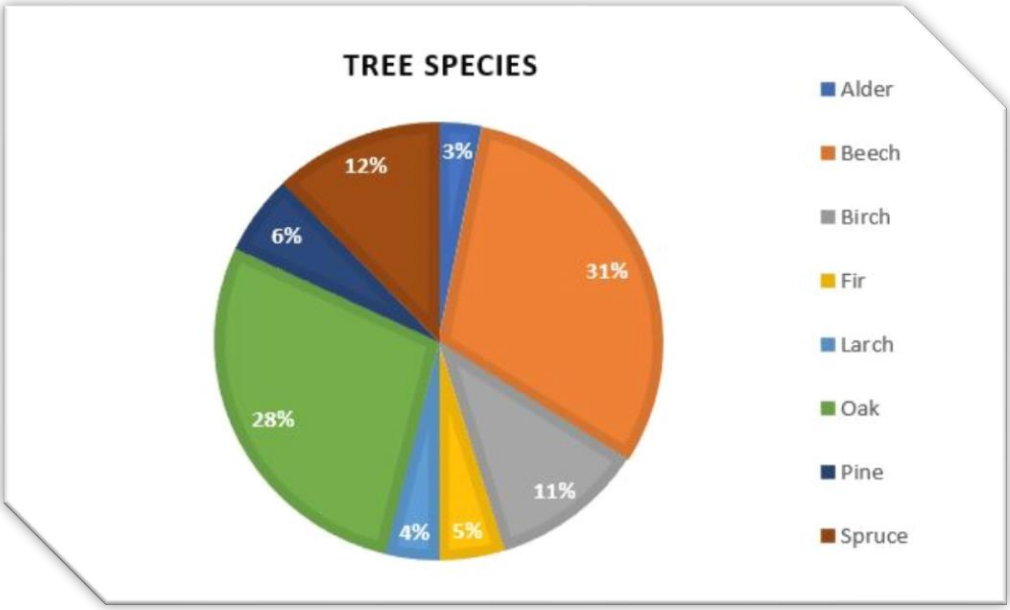

Figure 18: Type and Percentage of tree species.

4.1.2. Biometric DBH

The DBH of 544 trees were measured during the field survey, and results are presented in Figure 19. The mean DBH was 38 cm with a maximum and minimum of 82 and 10 cm, respectively. The field measured DBH was considered as a reference to predict the UAV based DBH and together with the Lidar tree height used to compute Lidar AGB.

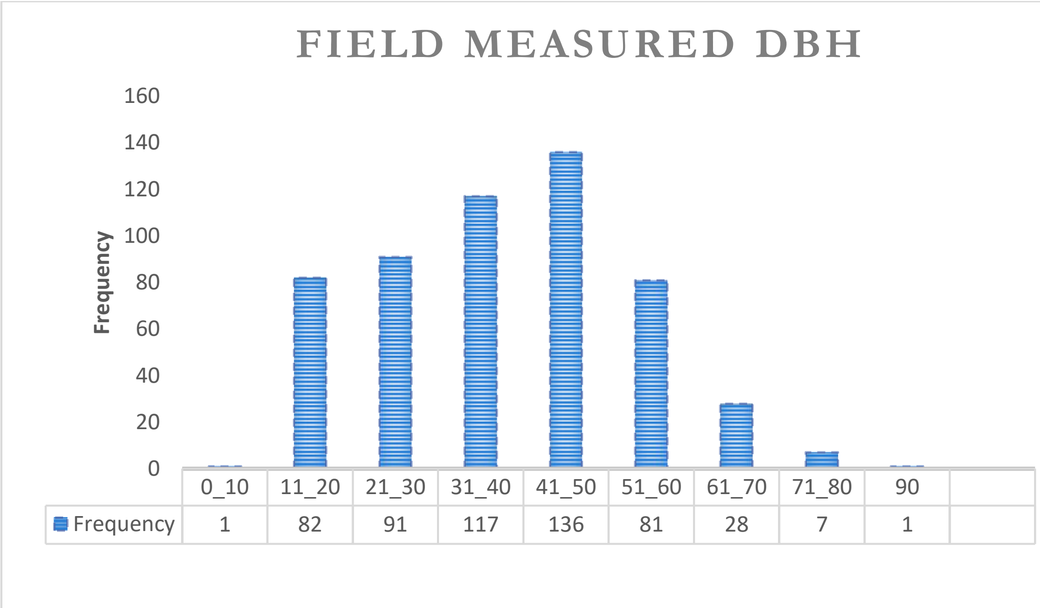

Figure 19: Frequency of field-measured DBH.

4.2. Accuracy assessment for UAV DTM of Leaf-on and Leaf-off Seasons

In this section, the accuracy assessment was made by comparing the UAV DTM of leaf-on and leaf-off seasons with the Lidar DTM. (Figure 20).

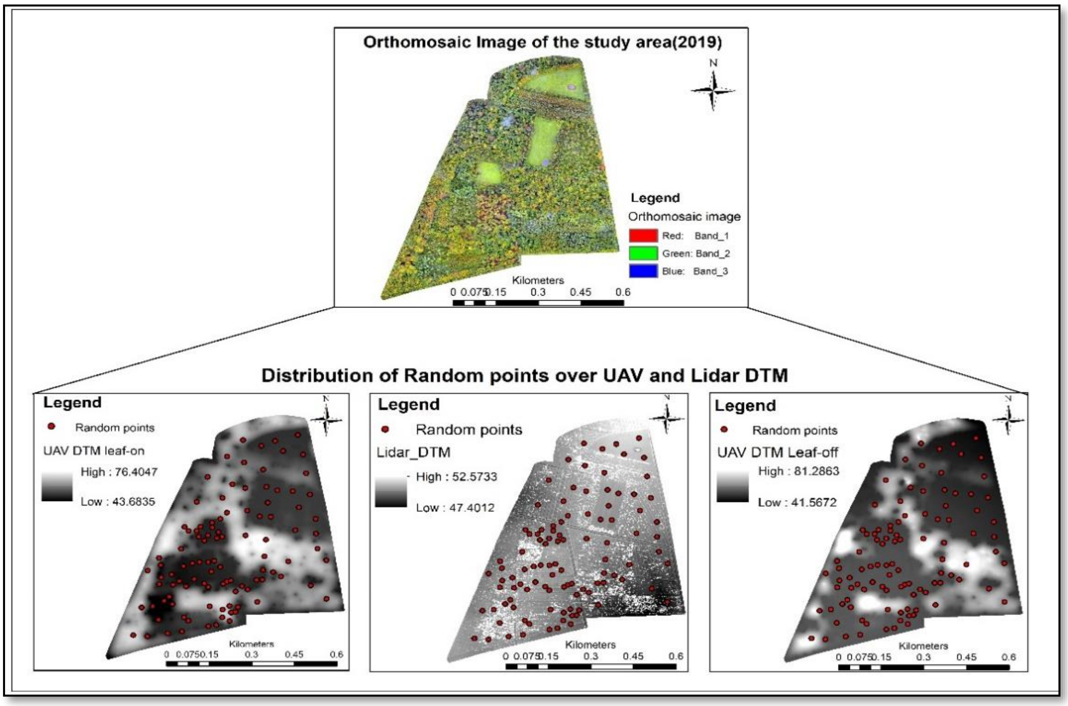

Figure 20: Distribution of random points over the UAV and Lidar DTM.

The coefficient of determination (R^2), the root mean square error (RMSE), and RMSE% were calculated for both seasons. The t-test is used to determine the difference between the UAV and Lidar datasets. F-test also was conducted to determine the type of t-test that need to be used. The details of the statistics are shown in Figure 21, and the descriptive statistics in Appendix 7.

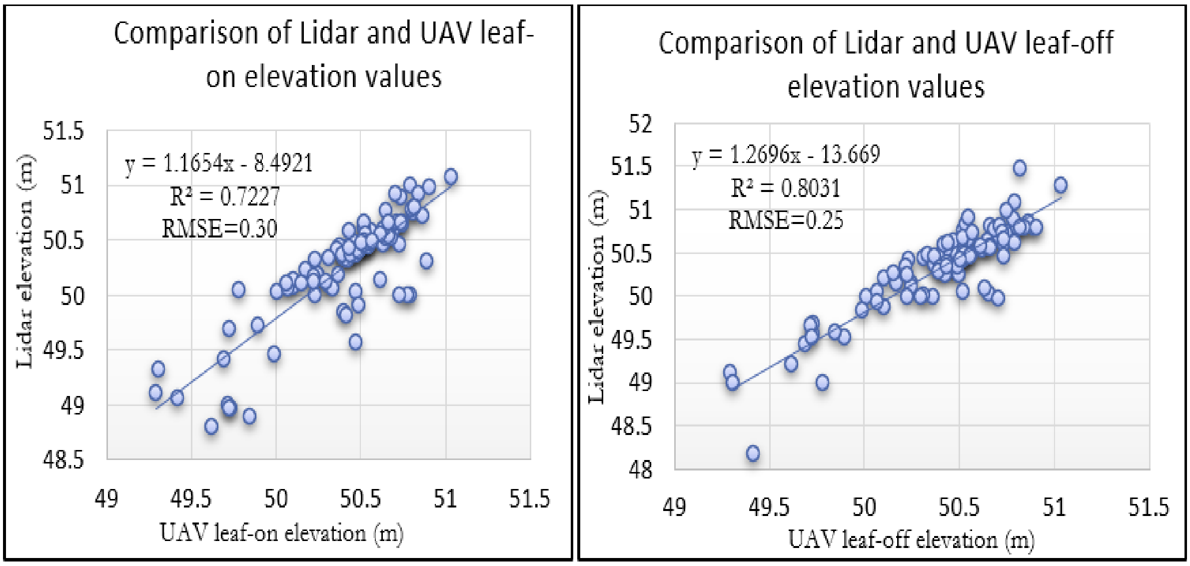

Figure 21: Comparison between Lidar and UAV Elevation points for both seasons.

The comparison of the result revealed that there is a strong relationship between Lidar and UAV DTM values. However, from the two UAV datasets, UAV leaf-off season have a stronger relationship with the Lidar, as is proven by its high R^2 value and low RMSE error produced. As demonstrated in Figure 21, the coefficient of determination (R^2) between UAV leaf- on and Lidar elevation values was 0.72, with the root mean square error (RMSE) of 0.30m. Similarly, the leaf-off season gave R^2 and RMSE of 0.8m and 0.25 m, respectively. From the comparison, 80% of the elevation values extracted from UAV leaf-off season has fitted with the Lidar elevation values, and 0.25m (25%) of error has been obtained. Similarly, 72% of the UAV leaf-on season values have fitted with the Lidar values and showed an error of 0.30m, which was equivalent to 30 %. The error estimated from the two UAV datasets has a difference of 5%. This indicates that the accuracy of DTM was improved by 5% during the leaf-off season.

The difference between Lidar and UAV elevation values was determined by conducting, t-test. But, F-test was performed before t-test to decide if the elevation values from Lidar and UAV had equal or unequal variance. The result of the F-test shown in Table 7.

Table 7: F-Test Two-Sample for Variances.

	Lidar	UAV leaf-off	Lidar	UAV leaf-on
Mean	50.40982	50.33212	50.40982	50.25772
Variance	0.128158	0.257242	0.128158	0.240874
Observations	100	100	100	100
df	99	99	99	99
F	0.498201		0.532055	
P(F<=f) one-tail	0.000309		0.000948	
F Critical one-tail	0.717329		0.717329	

Decision: F-Statistics < F-Critical (P <0.05), unequal variance

According to the result from the F-test, there was an unequal variance between Lidar and UAV leaf-on and leaf-off elevation values, because the p-values for both cases was less than the value of alpha 0.05, where F-statistics < F-Critical (p<0.05). Thus, t-test assuming unequal variance was conducted to determine if there is a significant difference or not between Lidar and UAV leaf-on and leaf-off elevation values. Result of the t-test is shown in Table 8.

Table 8: t-Test Two-Sample Assuming Unequal Variances.

	Lidar	UAV leaf-off	Lidar	UAV leaf-on
Mean	50.40982185	50.33212	50.40982	50.25772
Variance	0.128158064	0.257242	0.128158	0.240874
Observations	100	100	100	100
df	178		181	
t Stat	1.251685112		2.503752	
P(T<=t) one-tail	0.106163499		0.006587	
t Critical one-tail	1.653459126		1.653316	
P(T<=t) two-tail	0.212326998		0.013173	
t Critical two-tail	1.973380889		1.973157	

Similarly, t-test assuming unequal variance with alpha 0.05 and 95% confidence interval was applied, and the results are presented in Table 8. Results showed that the UAV leaf-on season has a p-value of 0.01 and the leaf-off season has 0.2. This proves that as there is no statistically significant difference between UAV and Lidar elevation values during the leaf-off season. In contrast, a significant difference was observed between UAV and Lidar DTM elevation values during the leaf-on season.

4.3. Tree heights extracted from CHM of Leaf-on and Leaf-off Seasons

In this section, the comparison was made between the tree heights derived from CHM of leaf-on and leaf-off seasons. The CHM for the leaf-on season is generated by subtracting the DSM and DTM of the leaf-on season. Wheres as the CHM for the leaf-off season was generated by combining the DSM and DTM of two different seasons images. The DSM is obtained from the image of leaf-on and DTM from the leaf-off season.

4.3.1. Descriptive statistics of UAV height for leaf-on and leaf-off seasons

As indicated in Table 9, the mean tree height derived from UAV images of leaf-on and leaf-off seasons were 15.9m and 17.6m, respectively. The mean tree heights difference between the two UAV datasets is about 1.6m. The tree heights computed from UAV image captured on the leaf-off season were a bit higher than the height of the leaf-on season. The minimum and maximum tree heights obtained from UAV image were 4.4m and 34.6m for the leaf-on season, whereas 3.5m and 37.3m for the leaf-off season. The two minimum and maximum tree heights have a difference of 0.9 and 2.7m, respectively. The median tree hight estimated during the leaf-on season is lower than a leaf-off season, as shown in Table 9.

Table 9: Descriptive Statistics of UAV tree heights for leaf-on and leaf-off seasons.

	Tree Height Leaf-on Season	Tree Height Leaf-off Season
Mean	15.95840321	17.60723715
Standard Error	0.283288042	0.293695653
Median	14.34910011	16.04600048
Standard Deviation	6.607355775	6.850100907
Sample Variance	43.65715033	46.92388244
Kurtosis	-0.642183485	-0.486989792
Skewness	0.557598153	0.539542756
Range	30.20438147	33.84780025
Minimum	4.424620152	3.503399849
Maximum	34.62900162	37.3512001
Sum	8681.371346	9578.337007
Count	544	544
Confidence Level(95.0%)	0.556474711	0.576918824

4.3.1.1. Conifer tree heights of leaf-on and leaf-off seasons

Table 10 shows descriptive statistics of conifer trees from leaf-on and leaf-off seasons. The statistics include all the conifer trees available under my study sample plots. Within in the selected sample plots, 124 tree species of spruce, Douglass fir and pine were found. The mean tree height of conifer tree was 17.4m and 19.2m for leaf-on and leaf-off seasons, respectively and the mean tree height difference was 1.4m. The minimum tree heights of leaf-on and off-seasons were 6.07 and 7.4m with maximum heights of 34.6 and 37.3m.

Table 10: Descriptive statistics of Conifer tree heights from both seasons.

	Conifer height (leaf-on)	Conifer height (leaf-off)
Mean	17.74131	19.20058
Standard Error	0.72733	0.754947
Median	15.99465	16.53455
Standard Deviation	8.099204	8.406729
Sample Variance	65.59711	70.67309
Skewness	0.396315	0.561488
Range	28.55303	29.94959
Minimum	6.07597	7.40161
Maximum	34.629	37.3512
Sum	2199.922	2380.872
Count	124	124
Confidence Level(95.0%)	1.439705	1.49437

4.3.1.2. Deciduous tree heights of leaf-on and leaf-off seasons

Table 11 shows the summary of statistics of deciduous tree height under my sample plots. It provides height information for 420 deciduous trees of species such as beech, birch, alder and larch, which are the most dominant and abundant trees in my study area as well as in my sample. The mean tree height of these species was 15.4m and 17.1m for leaf-on and leaf-off seasons. The difference between the two means is 1.7 m, which is higher compared to the mean deviation of conifer trees. The minimum and maximum tree height of leaf-on season were 4.4m and 31m and 3.5 and 32m for the leaf-off season.

Table 11: Descriptive statistics of deciduous trees for both seasons.

	Deciduous height (leaf-on)	Deciduous height (leaf-off)
Mean	15.43202	17.13682
Standard Error	0.293186	0.30508
Median	13.90477	15.8566
Standard Deviation	6.008517	6.25228
Sample Variance	36.10227	39.091
Skewness	0.460181	0.339086
Range	26.59648	29.4589
Minimum	4.42462	3.5034
Maximum	31.0211	32.9623
Sum	6481.449	7197.465
Count	420	420
Confidence Level(95.0%)	0.576298	0.599678

4.3.2. Comparing tree Heights from leaf-on and leaf-off seasons

A total of 544 both conifer and deciduous trees were used to make a comparison between tree heights derived from UAV CHM of leaf-on and leaf-off seasons. The scatter plot in Figure 22 demonstrated the relationship among tree height of leaf-on and leaf-off seasons. The two tree heights have a strong correlation observed with R^2 of 0.88. The root means square error (RMSE) between the two datasets was 2.2m.

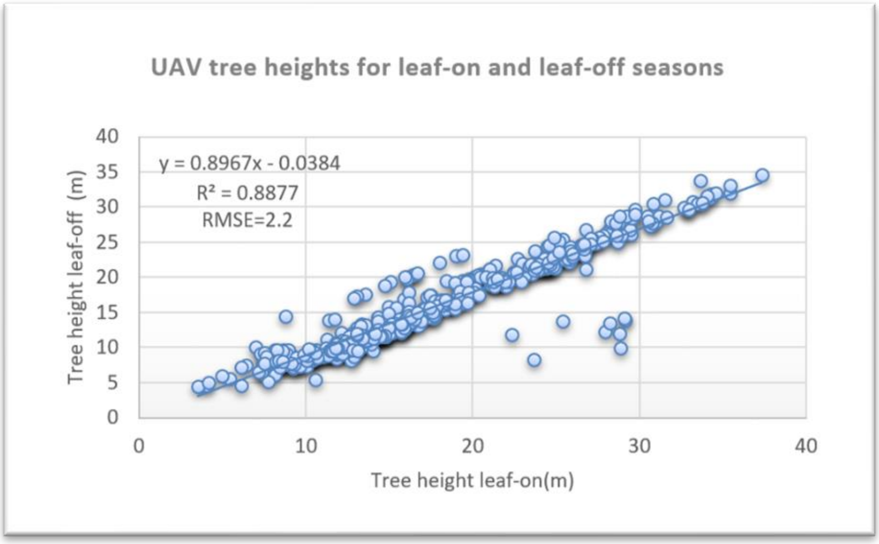

Figure 22: Tree heights from leaf-on and leaf-off seasons.

Additionally, F-test was performed to find if the two sample tree heights from leaf-on and leaf-off seasons have equal or unequal variance and to decide which type of t-test needs to be conducted. The F-test result is presented in Table 12.

Table 12: F-test Two-Sample for Variances.

	Tree height(leaf-off) season	Tree height(leaf-on)season
Mean	17.60724	15.9584
Variance	46.92388	43.65715
Observations	544	544
df	543	543
F	1.074827	
P(F<=f) one-tail	0.200379	
F Critical one-tail	1.151768	

Decision: F-statistic < F-critical (P> 0.05): Equal variance

Results show that the values of F-statistic and F-critical were 1.074827 and 1.151768, respectively. The two UAV RGB images acquired during the leaf-on and leaf-off seasons have the p-value of 0.200379. Thus, F-statistic < F-critical (P> 0.05) has equal variance. Therefore, t-test assuming equal variance was conducted.

Table 13: t-Test: Two-Sample Assuming Equal Variances.

	Tree height(leaf-off) season	**Tree height(leaf-on)season**
Mean	17.60724	15.9584
Variance	46.92388	43.65715
Observations	544	544
df	1086	
t Stat	4.04071	
P(T<=t) one-tail	2.85E-05	
t Critical one-tail	1.646258	
P(T<=t) two-tail	5.7E-05	
t Critical two-tail	1.962151	

Decision: F-statistic > F-critical (P< 0.05): there is a significant difference between the two means, and the null hypothesis was rejected.

4.4. CPA_DBH model development and validation

A total of 105 trees were randomly selected from 35 plots for model development and validation. The DBH of the chosen trees ranges from 13 to 80 cm and includes all types of tree species. Three trees were selected from each plot with their field measured DBH. From the selected 105 trees, 60% (63 trees) are used for model development, and the remained 40% (42 trees) are used for validation, respectively.

4.4.1. CPA_DBH model development

The linear, logarithm, power and quadratic models were used to test the relationship between the field measured DBH, and the CPA digitized from the orthophoto of UAV leaf-on season image (Figure 23).

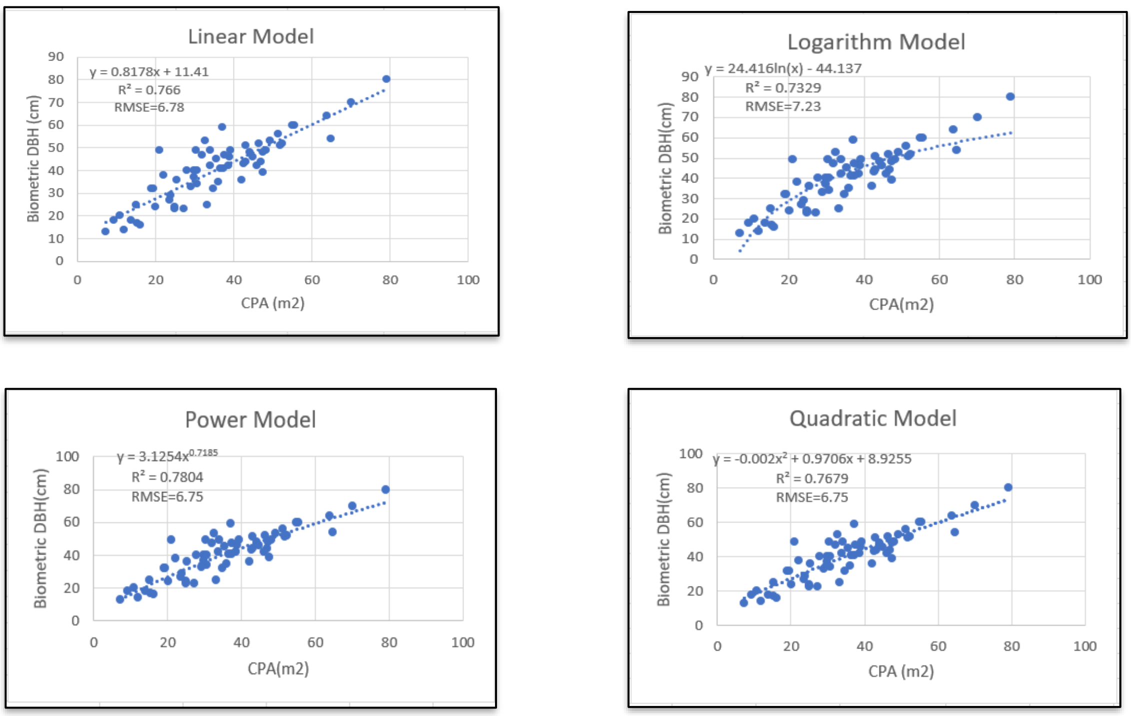

Figure 23: Regression models used to predict UAV_DBH using CPA and field measured DBH.

The result obtained indicated that the power model showed the highest R^2 compared to the other models. The power model produced R^2 values of 0.78 and followed by the quadratic model, which is 0.76. The linear model has produced nearly the same result with the quadratic model. Regarding the RMSE error, the power and quadratic model gave the same result. Based on the result obtained, the power model is selected to model the UAV - DBH relationship.

Table 14: Regression equations used for model development.

Model	Equations	R2	RMSE(cm)
Linear	DBH=0.8178*CPA+11.41	0.766	6.782923044
Logarithm	DBH=24.416*ln(CPA)-44.137	0.7329	7.245878717
Power	DBH=3.1254*(CPA)^0.7185	0.7804	6.745645938
Quadratic	DBH=-0.002*(CPA)²+0.9706*CPA+8.9255	0.7679	6.754342

4.4.2. Model validation and accuracy

The equation obtained from the power model (DBH=3.1254*(CPA)^0.7185) was used to model the UAV-DBH (Figure 24). From randomly selected 105 trees, 40% (42) are used for validation. These trees are selected from each plot, and their DBH ranges from 12 to 69 cm.

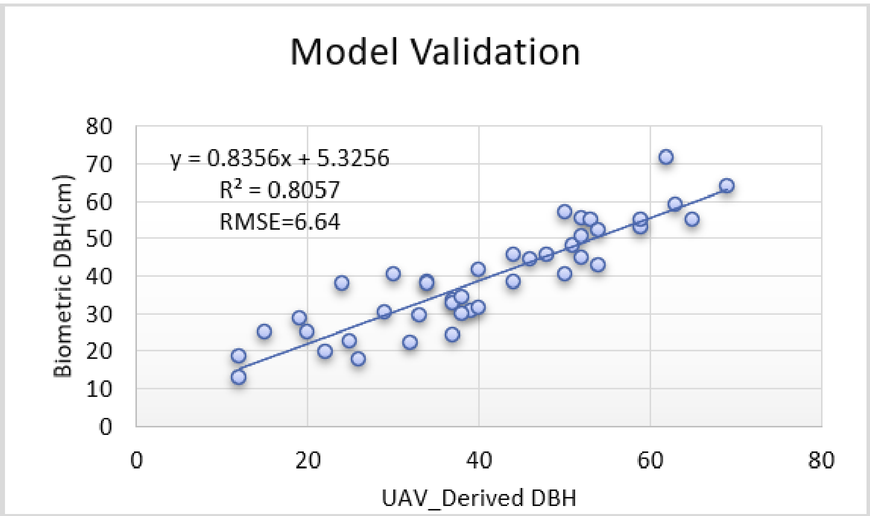

Figure 24: Scatter plot of model validation of UAV-DBH.

The validation results revealed that about 80% per cent of the field measured DBH was well fitted with modelled DBH with R^2 of 0.8 and RMSE of 6.64cm. Moreover, a strong positive correlation was observed between the measured DBH and the CPA of the tree. Therefore, there is a significant relationship between CPA segmented from UAV image and DBH measured in the field and the null hypothesis was rejected

4.5. Above Ground Biomass and Carbon estimation

Above-ground biomass (AGB) and aboveground carbon (AGC) were estimated from Lidar and UAV datasets. The tree heights derived from UAV RGB images of 2019 (leaf-on) and 2020 (leaf-off) seasons were used as an input to estimate the AGB and carbon stock for the year 2020. On the other hand, the predicted UAV DBH from crown projection area (CPA) of leaf-on season image was combined with the leaf-on and leaf-off season tree heights to estimate the AGB and AGC. The AGB from Lidar data was estimated using tree height obtained from the Lidar CHM and biometric DBH. The AGB/AGC of each tree species was calculated based on the allometric equations obtained from (Zianis et al., 2005). All the allometric equations, developed for Dutch forest (site and species-specific equations), were used to quantify the biomass.

The total AGB estimated from UAV datasets were 519 and 476 Mg/ha for a leaf on and leaf-of season, respectively whereas 566 Mg/ha was estimated from the Lidar data. The AGB estimated from the Lidar data was found to be higher than the UAV result, followed by UAV leaf-off season. The minimum and maximum AGB estimated from the leaf-off season was 0.011313619 and 4.523501661Mg/tree and 0.011058677 and 4.201384026 for the leaf-on season. Lidar has a minimum and maximum AGB of 0.014186373 and 4.522775558 (Table 15).

Table 15: Descriptive Statistics for UAV Leaf-on and leaf-off seasons and Lidar AGB Mg/tree.

	AGB-Lidar (Mg/tree)	**AGB UAV leaf-off (Mg/tree)**	**AGB UAV Leaf-on (Mg/tree)**
Mean	1.042104728	0.954442647	0.872190517
Standard Error	0.034534661	0.035548301	0.032822837
Median	0.901765163	0.714861295	0.666218198
Standard Deviation	0.805479793	0.829121727	0.765553544
Sample Variance	0.648797697	0.687442838	0.586072229
Range	4.508589184	4.512188042	4.190325349
Minimum	0.014186373	0.011313619	0.011058677
Maximum	4.522775558	4.523501661	4.201384026
Sum	566.904972	519.2167999	476.4716413
Count	544	544	544
Confidence Level(95.0%)	0.067837899	0.069829034	0.064475291

The conversion factor 0.47, which is recommended by (IPCC, 2006) was used to convert the AGB estimated from Lidar and UAV datasets to AGC. The total AGC estimated from Lidar data was 266Mg/ha, and 223 and 244 Mg/ha from leaf-on and leaf-off seasons. Similar to AGB, the AGC estimated from the Lidar data was found higher than both UAV datasets. The minimum and maximum AGC for Lidar data were 0.006667596 and 2.125704512.

The UAV leaf-on season has a minimum and maximum of 0.005197578 and 1.974650492 Mg per/tree as well as 0.005317401 and 2.126045781 Mg/tree for the leaf-off season (Table16). In general, the Lidar and UAV leaf-off season were shown better estimation respectively on both AGB and AGC. The AGB/AGC estimated at tree level are organized in plot-level, as shown in Appendix 6, Figure 25 and 26.

Table 16: Descriptive Statistics for UAV and Lidar AGC Mg/tree.

	Lidar_AGC (Mg/tree)	AGC_UAV leaf-off (Mg/tree)	AGC_UAV leaf-on (Mg/tree)
Mean	0.489789222	0.448588044	0.409929543
Standard Error	0.016231291	0.016707701	0.015426734
Median	0.423829627	0.335984809	0.313122553
Standard Deviation	0.378575503	0.389687212	0.359810166
Sample Variance	0.143319411	0.151856123	0.129463355
Range	2.119036917	2.12072838	1.969452914
Minimum	0.006667596	0.005317401	0.005197578
Maximum	2.125704512	2.126045781	1.974650492
Sum	266.4453369	244.031896	223.0016714
Count	544	544	544
Confidence Level(95.0%)	0.031883813	0.032819646	0.030303387

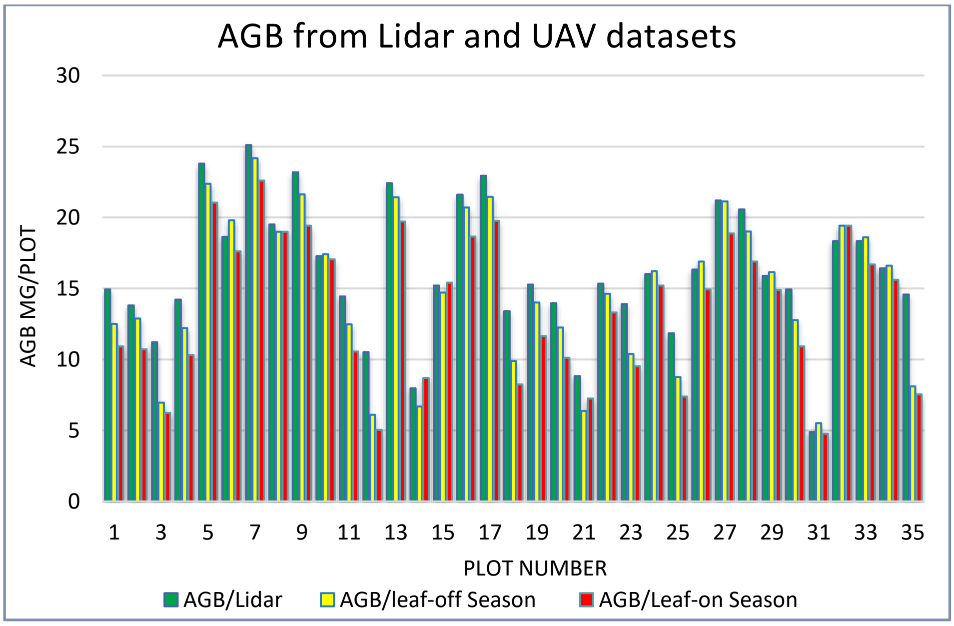

Figure 25: Comparison of AGB from Lidar and UAV datasets.

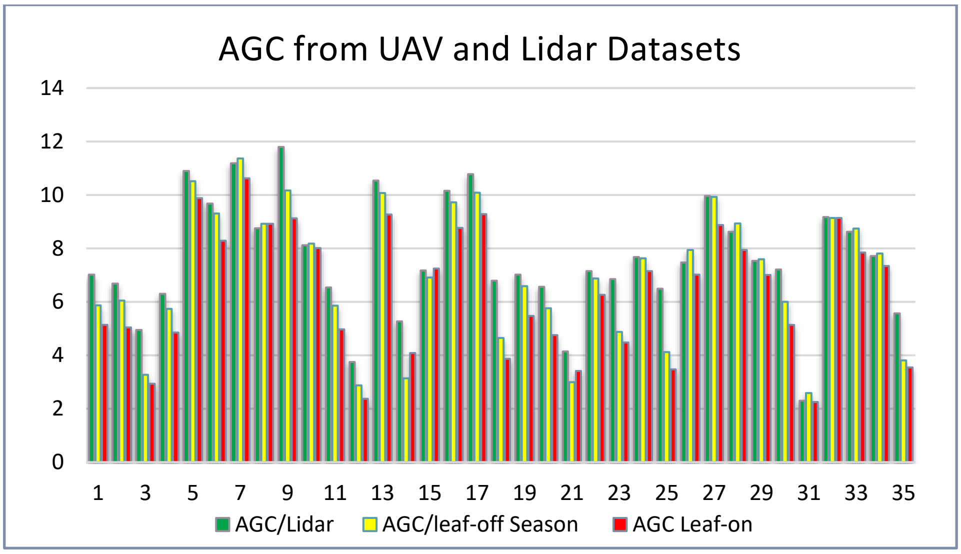

Figure 26: Comparison of AGC from Lidar and UAV datasets.

As indicated in Figure 25 and 26, the highest AGB/AGC in most of the plots was estimated from the Lidar data. But the AGB/AGC also equally estimated from UAV leaf-on and leaf-off seasons in plot 8. Under plots 6, 10, 16, 26, 31 and 33 found a bit higher for UAV leaf-off season than the others. In plots 14 and 15 AGB/AGC leaf-on season was overestimated. The highest estimated AGB and AGC from the Lidar data was 25 and 11.3Mg/ha under plot 7. At the same time, the lowest estimated AGB and AGC was 4.7 and 2.2 Mg/ha from UAV leaf-on season under plot 31.

4.5.1. Comparison of AGB and AGC from UAV datasets

The comparison was made between AGB and AGC estimated from UAV RGB images of leaf-on and leaf-off seasons. As Figure 27 shows the scatter plot, both the AGB and AGC estimated from the leaf-on and leaf-off season have shown a strong correlation. They produced R^2 of 0.96 and RMSE of 0.13 and 0.06 Mg/tree for both AGB and AGC respectively.

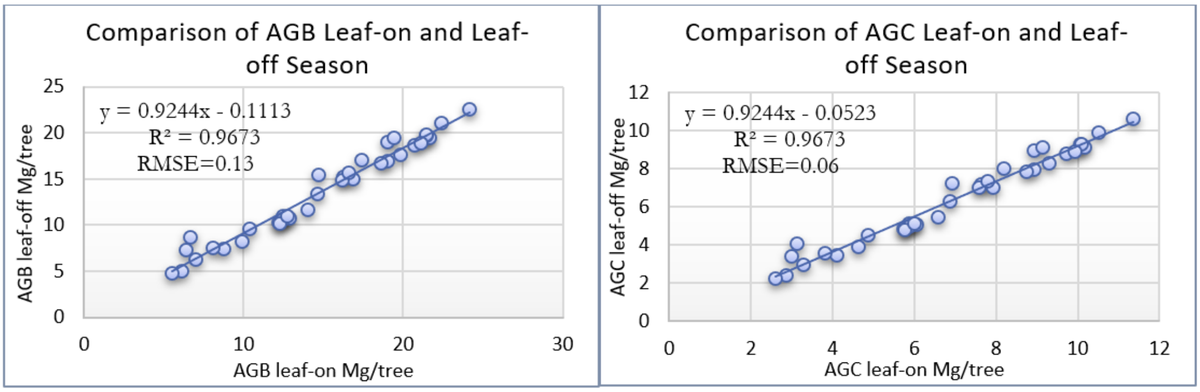

Figure 27: AGB/AGC for UAV leaf-on and leaf-off seasons.

To test the significance of the relationship among AGB estimated from leaf-on and leaf-off season, the F-test and the t-test were performed. The F-test was conducted to find out if the estimated AGB from leaf-on and leaf-off seasons has an equal or unequal variance. The F-test result is shown in Table 17.

Table 17: F-Test Two-Sample for Variances.

	AGB leaf-off season	AGB leaf-on season
Mean	0.95444265	1.741180335
Variance	0.68744284	412.1380954
Observations	544	544
df	543	544
F	0.00166799	
P(F<=f) one-tail	0.001	
F Critical one-tail	0.86828194	

Thus, t-test with unequal variance at alpha 0.05 and 95% confidence interval was used to test their significance.

Table 18: t-Test: Two-Sample Assuming Unequal Variances.

	AGB leaf-off season	AGB leaf-on season
Mean	0.954442647	0.872190517
Variance	0.687442838	0.586072229
Observations	544	544
df	1079	
t Stat	1.699982921	
P(T<=t) one-tail	0.044711167	
t Critical one-tail	1.646267053	
P(T<=t) two-tail	0.089422334	
t Critical two-tail	1.962164994	

Decision: F-statistics<F-Critical (P >0.05): There is no significant difference in AGB estimated from UAV leaf-on and leaf-off season. Therefore, the null hypothesis is accepted because the p-value is greater than alpha (0.05).

4.5.2. Comparison by forest type

Figure 28 shows a comparison of AGB for conifer and broad leaf-trees separately. AGB of conifer trees estimated from leaf-on and leaf-off seasons are compared to each other to check how they fit and deviate to each other. The comparison of conifer includes 124 trees with three different species type. The obtained result has shown R^2 and RMSE of 0.97 and 0.15 Mg/tree, respectively. The AGB for broad-leaf trees was estimated from 420 trees. The result has produced R^2 and RMSE of 0.95 and 0.2 Mg/tree. Compared to the broad-leaf trees, the AGB estimated for conifer trees from both seasons has shown better fit and the error is lower. This indicated the seasonal variation has less effect on conifer trees compared to the deciduous trees.

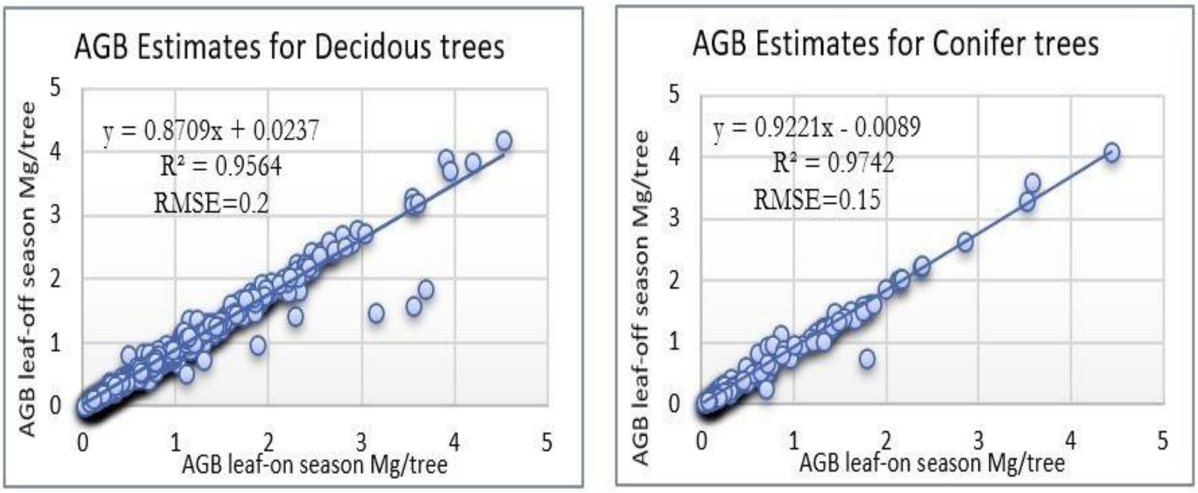

Figure 28: Comparison of AGB by forest type.

Furthermore, to test if there is a significant difference between AGB of conifer and broad-leaf trees from the leaf-on and leaf-off seasons, the F-test and t-test were conducted separately Table 19.

Table 19: F-Test Two-Sample for Variances.

	Conifer Leaf-off	Conifer Leaf-on	Broadleaf Leaf-off	Broadleaf-Leaf-on
Mean	0.995936	0.907588	0.8139	0.752295
Variance	0.694347	0.587613	0.643722	0.566819
Observations	420	420	124	124
df	419	419	123	123
F	1.18164		1.135675	
P(F<=f) one-tail	0.043985		0.240766	
F Critical one-tail	1.174562		1.346856	

Based on the result from the F-test conifer and broadleaf-trees has p-values of 0.04 and 0.2 respectively. Therefore t-test assuming unequal variance was conducted for conifer trees and t-test assuming equal variance was used for deciduous trees.

Table 20: t-Test: Two-Sample Assuming Equal Variances.

	Deciduous leaf-off	Deciduous leaf-on
Mean	0.995936	0.907588
Variance	0.694347	0.587613
Observations	420	420
df	838	
t Stat	1.599128	
P(T<=t) one-tail	0.055085	
t Critical one-tail	1.646674	
P(T<=t) two-tail	0.110169	
t Critical two-tail	1.962799	

Table 21: t-Test: Two-Sample Assuming Unequal Variances.

	Conifer Leaf-off	Conifer Leaf-on
Mean	0.8139	0.752295
Variance	0.643722	0.566819
Observations	124	124
df	245	
t Stat	0.623506	
P(T<=t) one-tail	0.266766	
t Critical one-tail	1.651097	
P(T<=t) two-tail	0.533532	
t Critical two-tail	1.969694	

Decision: F-statistics<F-Critical (P >0.05): There is no significant difference in AGB estimated from leaf-on and the leaf-off season for both conifer and broad-leaf trees.

4.6. Accuracy assessment of UAV derived AGB compared to Lidar AGB

In this section, the accuracy of UAV derived AGB was assessed compared to AGB from the Lidar data. The AGB comparison between Lidar and UAV leaf-on season has produced R^2 and RMSE of 0.86 and 0.724 Mg/tree. At the same time, the R^2 and RMSE from UAV leaf-off season were 0.91 and 0.72 Mg/tree. The AGB result estimated from both UAV datasets has shown a strong positive correlation. But, the UAV leaf-off season has shown a better fit compared to the UAV leaf-on (Figure 29).

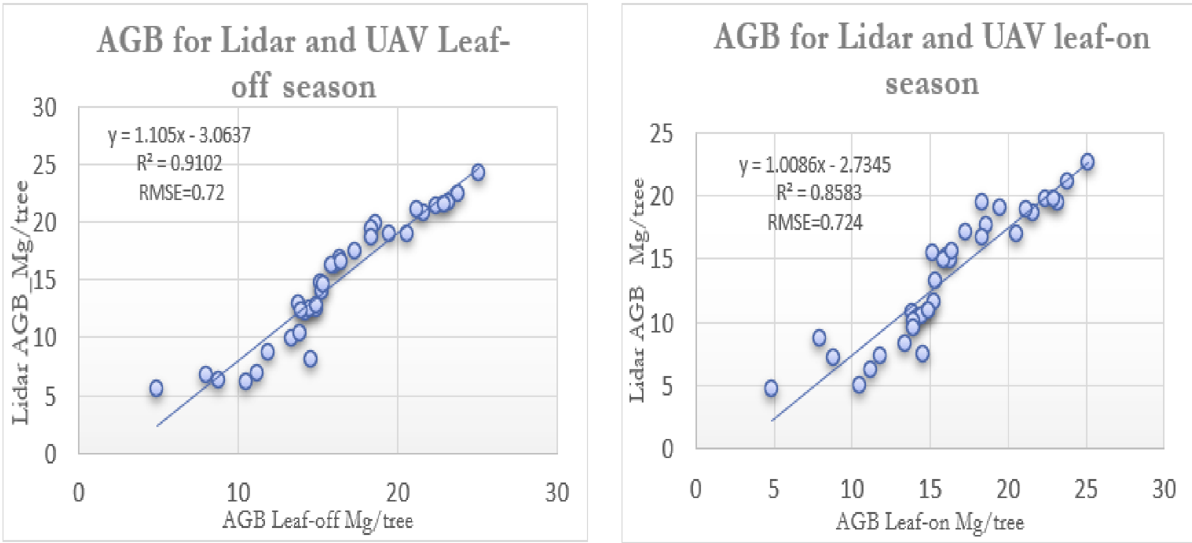

Figure 29: Comparison of Lidar and UAV derived AGB and AGC.

To see if there is a significant difference between AGB from Lidar and UAV datasets t-test was performed. But, before the t-test, the F-test was conducted first to decide which t-test needs to be used.

Table 22: F-Test Two-Sample for Variances.

	Lidar AGB	AGB Leaf-off	Lidar AGB	AGB Leaf-on
Mean	1.042105	0.954443	1.042105	0.872191
Variance	0.648798	0.687443	0.648798	0.586072
Observations	544	544	544	544
df	543	543	543	543
F	0.943784		1.107027	
P(F<=f) one-tail	0.250234		0.118233	
F Critical one-tail	0.86823		1.151768	

The p-value from F-test table was 0.2 and 0.1 for UAV leaf-off and leaf-on season respectively. These obtained values were higher than the value of alpha (0.05) (Table 22). Therefore t-test assuming equal variance was conducted for both.

Table 23: t-Test: Two-Sample Assuming Equal Variances.

	Lidar_AGB	AGB Leaf_off	Lidar_AGB	AGB Leaf-on
Mean	1.042105	0.954443	1.042105	0.872191
Variance	0.648798	0.687443	0.648798	0.586072
Observations	544	544	544	544
df	1086		1086	
t Stat	1.76876		3.566306	
P(T<=t) one-tail	0.038607		0.000189	
t Critical one-tail	1.646258		1.646258	
P(T<=t) two-tail	0.077215		0.000378	
t Critical two-tail	1.962151		1.962151	

Case1.Decision: t-Statistics < t-Critical (P > 0.05): There was no significant difference observed between the two means.

Case2. Decision: t-Statistics > t-Critical (P < 0.05): There was a significant difference observed between the two means.

5. DISCUSSION

5.1. Accuracy Assessment of UAV DTM compared to Lidar DTM

The Digital Terrain Model (DTM) is a significant topographic product, which has an essential demand for many applications. Previously the traditional methods were used to create DTM, which was costly and time-consuming because of land surveying (Polat and Uysal, 2018). Overtime, UAV Photogrammetry started to become one of the significant techniques to generate DTM. Nowadays, airborne Light Detection and Ranging (Lidar) technology have appeared as a powerful method to create DTM. Lidar has the advantage of collecting 3D information over large areas very efficiently and accurately (Polat & Uysal, 2018). The Lidar technology can penetrate and look through gaps in vegetation canopies and reach the ground surface. This makes Lidar register multiple returns which represent the canopy and the terrain (Moudry et al., 2019). Whereas a large portion of ground information is missing in the forest areas when using UAV photogrammetry or SfM technique, this is due to blocking caused by the canopy of the tree. Moreover, Lidar DTM data is a measurement output while UAV DTM is an estimation or inferential output of using SfM of several 2D images. Due to these reasons, the DEM data derived from UAV photogrammetry is not highly reliable compared to the Lidar (Huang et al., 2019).

Various factors are affecting the accuracy of the DTM: vegetation coverage (the canopy density); undergrowth, shrubs, and grasses; the terrain of the surface; filtering and other related algorithms used during image processing (Huang et al., 2019; Moudry et al., 2019) stated the difficulty of acquiring accurate DTM under dense vegetation canopy forests. The pix4d image processing result obtained from the quality report of this study proves the claim of Huang, (2019). The canopy density affects the density of point cloud generated over the area. The images captured from the leaf-on and leaf-off seasons have shown the different point of cloud densities. The more the canopy is open, the more points are created and vice versa. Table 24 showed point cloud generated within the study area and average density of points/m^2 during the leaf-on and leaf-off seasons.

Table 24: Point cloud density during leaf-on and leaf-off seasons.

Number	Leaf-on	Leaf-off
Number of Generated Tiles	4	4
Number of 3D Densified Points	61138701	74539481
Average density (per m2)	30.3	33.05

According to the information from Table 24, 61138701 3D-densified points were created within the study area during the leaf-on season with the average point density of 30.3 per /m^2. At the same time the leaf-off season has shown 74539481 3D-densified points and 33.05 average density of points per/m^2. The point density for the leaf-off season was significantly higher than the leaf-on season. Figure 30, shows the density of point cloud from a small part of the study area for the two seasons. Letter 'A' and 'C' shows the density of points cloud and some parts of orthophoto during the leaf-on season and 'B' and 'D' for the leaf-on season. As clearly shown in Figure 30 'B' and 'C' dense point clouds were generated due to open canopy for the leaf-off season and vice versa.

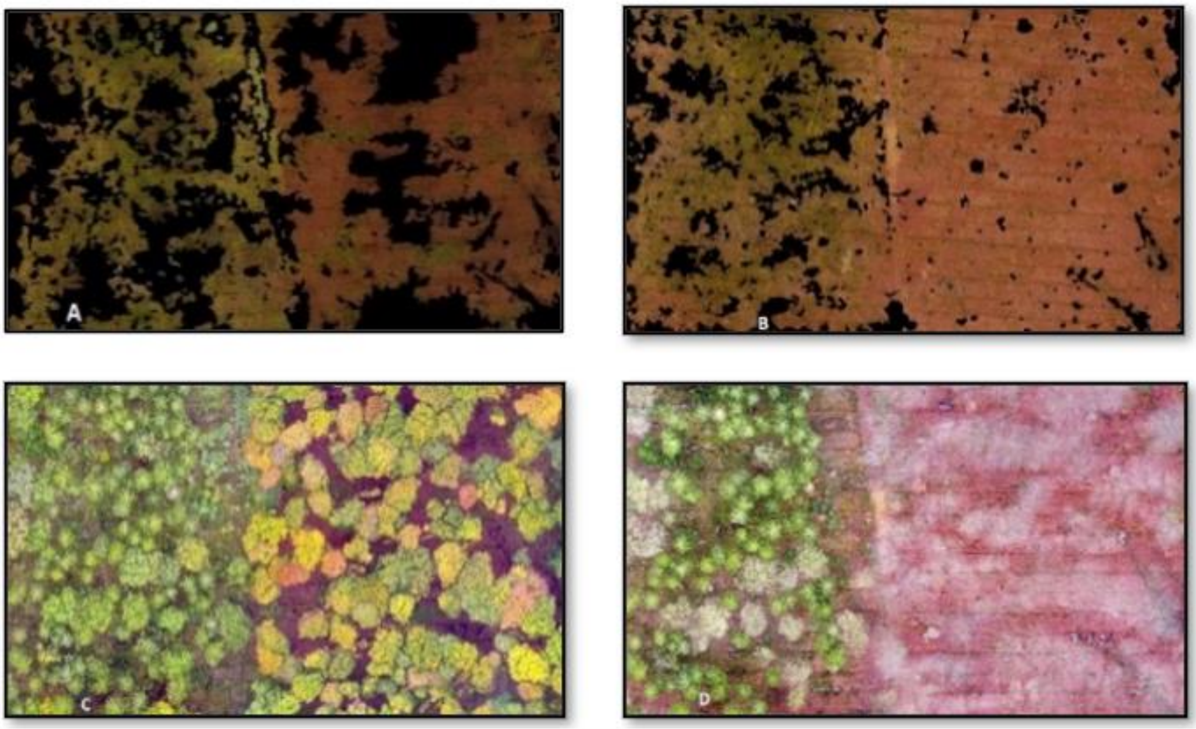

Figure 30: Visual comparison of ground point densities from leaf-on (A, C) and leaf-off (B, D) seasons.

In this study, the elevation values extracted from the UAV photogrammetry DTM of leaf-on and leaf-off seasons and Lidar DTM were compared. The comparison was made using 100 random points, which were derived from both Lidar and UAV DTM. The values obtained from Lidar DTM was used as a reference to validate the values from UAV datasets.

The DTM accuracy assessment results from Lidar with UAV leaf-off season showed that R^2 and RMSE of 0.8 and 0.25m respectively, and the error is estimated around 25%. At the same time, the accuracy assessment made between Lidar and UAV leaf-on season showed R^2 and RMSE values of 0.72 and 0.30m with 30% of estimated error. Based on the result obtained, we concluded that the accuracy assessment of UAV DTM of the two seasons with Lidar has a strong correlation. But, the result of the UAV leaf-off season is more reliable as compared to the leaf-on season. The UAV leaf-off season has better accuracy compared to leaf-on season. This is due to the impact of the season on the tree canopy. But the level of error obtained from both UAV datasets was not that far to each other. This is highly related to the topography of the study area, which is generally a very flat and uniform surface. It also related to the nature of the forest, which is not dense and has mixed species, some of them are affected by seasonal change.

Some research works indicated that the accuracy of the DTM produced by UAV images varies from season to season. Huang et al. (2019) stated that the more accurate result is obtained in winter seasons, where most of the deciduous trees are shade their leaves and with low canopy coverage. On their study, they assessed the value of photogrammetric and Lidar-derived data. They collected the UAV imagery of different seasons. They evaluated whether the accuracy of SfM-derived DTMs can be improved by the acquisition of images under leaf-off conditions. As indicated on their result, lower accuracy was obtained in the leaf-on (summer) season while the result from leaf-off season image was found very accurate, and the resulted RMSE were 0.19m and 1.71m for leaf-off and leaf-on season respectively. They also stated that satellites images captured during the leaf-off season were comparable to the Lidar derived DTM. Similarly, this result also comparable with the works from Dandois and Ellis (2013). In their study, they assessed the accuracy of photogrammetric DTM compared to the Lidar data. The result obtained showed that DTM accuracy was highest during the leaf-off season, in which RMSE ranges between 0.7m to 2.72m. At the same time, RMSE error for leaf-on season ranges between 3.37m to 5.69m.

5.2. UAV leaf-on and leaf-off seasons heights comparison

Tree height is an essential forest parameter to estimate tree growth, forest volume and biomass, carbon stock and forest productivity, which are most important factors for the mitigation of climate change and ecological balance (Ganz et al., 2019). Tree height has been measured using direct and indirect methods. Recently using Unmanned Aerial Vehicle (UAV) remote sensing technologies are becoming preferred options to acquire reasonably accurate tree heights (Krause et al., 2019).

Descriptive statistics of this research were conducted for 544 trees which both heights derived from UAV CHM of leaf-on and leaf-off seasons. The mean tree height of 15.9 and 17.6m was estimated for leaf-on and leaf-off seasons, respectively. The maximum and minimum height for the leaf-on season was 34.6 m and 4.4m and 37.3m and 3.5m for the leaf-off season. In this study, two different photogrammetric tree height derived from leaf-on and leaf-off seasons were compared to show how they deviate to each other (n = 544). From the comparison made a very low amount of error was observed with R^2 and RMSE of 0.88 and 2.2 m respectively, which show that tree height measurements explain 88% of the variation in height measurement in UAV leaf-on season from leaf-off season data. The comparison showed a very high correlation between the two photogrammetric datasets. The obtained RMSE value indicates that as there is 2.2m height difference between height estimated from leaf-on and leaf-off seasons. In this study, t-test assuming equal variance was conducted to test if there is a significant difference between the two UAV datasets. From the result, a p-value less than alpha 0.05 was observed in which F-statistic > F-critical ($P < 0.05$). Thus, the obtained result reveals a statistically significant difference between the mean stand heights estimated from the UAV datasets (leaf-on and leaf-off seasons), and therefore, the null hypothesis was not accepted.

This result has some kinds of similarity with the study conducted by Krause et al., (2019). In their study, they compared 253 trees from two different seasons of UAV image. The study revealed very low RMSE error (0.138 m). The result of their comparison showed a very high correlation between the two photogrammetric data sets which resulted in R^2 values of 0.993. However, the study conducted by (Huang et al., 2019) has a contradicting idea compared to my result. In their study, the result showed improvement of accuracy during the leaf-on season, and they provide evidence as leaf-on conditions have a positive effect on tree height estimation. They also mentioned that as it is difficult to reconstruct the 3D canopy structure from UAV images of the leaf-off season and that leads to an underestimation of trees heights. In their study, they also indicated that the reduction of error (RMSE) from 2.894 and 1.433 m (leaf-off) to 0.729 and 0.597 m (leaf-on) respectively.

In this study, further analysis was made to give descriptive statistics of conifer and deciduous trees from the two separate seasons. The descriptive statistics were provided for 420 deciduous tree species of beech, birch, alder and larch. These deciduous trees were one of the most dominant and abundant tree species in the study area. From these results, the beech and the oak trees cover the most significant percentage. The summary statistics showed 31m and 4.4m maximum and minimum deciduous tree heights from leaf-on, whereas 32m and 3.5 and for the leaf-off season. The mean tree heights were 15.4m and 17.1m for leaf-on and leaf-off seasons, respectively. There is 1.7m height difference between the mean deciduous tree height of leaf-on and leaf-off season. The descriptive statistics for conifer species includes 124 trees, which includes three different species of spruce, Douglass fir and pine. The mean tree height was 17.4m and 19.2m for leaf-on and leaf-off season. The maximum and minimum tree heights were 34.6 and 6.07 for the leaf-on season and 7.4m and 37.3m for the leaf-off season. The mean tree height difference between conifer trees of the two seasons was 1,4m, which is lower than the mean height difference of the deciduous trees and has less season influence.

5.3. CPA_DBH model development and validation

The data for this analysis were collected from 35 plots, and 105 trees were chosen. The DBH of the identified trees ranges were from 13 to 80 cm with different species of conifer and deciduous trees. It includes deciduous species of beech, birch, larch, oak, and alder and conifer species of Norway spruce, Douglas fir and scot pine. The selected trees were randomly split into two groups to use it for both model development and validation. From the total of 105 trees, 60% or 63 trees were used to develop the model, and the remained 40% or 42 trees used for model validation. The selected regression models are linear, logarithm, power and quadratic. From the result, all the candidate regression models showed a good performance in explaining CPA-DBH relationship.

From the result, a strong positive and significant relationship was observed between the crown projection area of the tree diameter at breast height. The power model has resulted in an R2 value of 0.78 compared to the remained four models. The root means square error (RMSE) produced by power model was 6.74 cm, and the error estimated from the quadratic model is very close to the error of the power model, which was

6.75 cm. Therefore the power model was selected among the proposed four models because of its highest predictive power and low RMSE error and used to establish a relationship between CPA and DBH in the temperate forest ecosystem. The validation between CPA and DBH was made using the selected 42 trees, and the equation derived from the power model(DBH=3.1254*(CPA)^0.7185). The validation result revealed that about 80% per cent of the field measured DBH was well fitted with modelled DBH with R2 of 0.8 and RMSE of 6.64 cm. Moreover, a strong positive correlation was found between the measured DBH and the CPA of the tree.

Shimano (1997) also mentioned as the power model was the best to develop the relationship between CPA and DBH of the tree in deciduous and conifer forest. The model assumes that the increment of the CPA decreases as the DBH increases. On his study (Shimano, 1997), found R^2 of 0.93 and 0.87 for deciduous and conifer trees, respectively. The outcome of my result for CPA-DBH relationship was found in line to his study.

5.4. AGB and AGC

Above-ground biomass (AGB) was estimated using the allometric equations obtained from (Zianis et al., 2005). These equations were site and species-specific which was only developed to quantify the biomass in Dutch forests. Daba and Soromessa (2019) stated that the use of species and site-specific allometric equation used to quantify the AGB in higher accuracy. Therefore in this study, eight different sites and species-specific allometric equations were used to reduce error which might cause by environmental variation. The selected equations were used both height and tree DBH as its parameter. The inputs used for AGB estimation are taken from three different datasets. The predicted DBH combined with the tree heights derived from UAV leaf-on and leaf-off seasons were used as an input to compute AGB for leaf-on and leaf-off seasons. At the same time, the biometric DBH together with the Lidar derived height, were used to estimate AGB from Lidar. In general tree parameters derived from 544 trees were used as an input to estimate the AGB for this study.

The total AGB computed using tree parameters derived from Lidar and UAV leaf-on and leaf-off seasons were 566, 519 and 476 Mg/ha for Lidar, UAV leaf-off and leaf-on season respectively. The AGB computed from Lidar was found higher than UAV derived AGB. But, the difference was small with UAV leaf-off season than the leaf-on season. The Lidar derived AGB has a difference of 43 Mg from the UAV leaf-off season and 90 Mg from the leaf-on season. The carbon stock from Lidar and UAV datasets were computed by applying the conversion factor 0.47 as proposed by (IPCC, 2006). The converted AGC for Lidar and UAV leaf-on and leaf-off seasons were 266, 223 and 244 Mg/ha respectively.

The estimated AGB/AGC from UAV leaf-on and the leaf-off season was compared with each other by establishing the scatter plot. The obtained R^2 was 0.96 and with RMSE of 0.13 and 0.06 Mg/tree for both AGB and AGC respectively. The results indicated that the forest AGB /AGC computed from UAV datasets were highly correlated. Unequal variance t-test also was conducted to test the significance of the relationship between AGB/AGC obtained from the UAV datasets. The result gave p-values of 0.08, which was higher than the p-values of alpha (0.05). This proves as there is no significant difference between AGB and AGC from the two UAV datasets, and the null hypothesis was accepted. Further analysis also made to see the relationship of AGC/AGC in different forest types. The scatter plot made for deciduous trees showed R^2 and RMSE of 0.95 and 0.2 Mg/tree. At the same time, R^2 between AGB of conifer trees from the leaf-on and leaf-off seasons were 0.97 with RMSE of 0.15 Mg/tree. The p-value result from t-test were 0.1 and 0.5 for deciduous and conifer trees, respectively. The p-values for both cases were found higher than alpha 0.05. Therefore, a significant difference was not observed between deciduous and conifer trees from leaf-on and leaf-off seasons and the null hypothesis were accepted.

The accuracy assessment was made by comparing the AGB derived from UAV datasets by taking the Lidar AGB as reference. The scatter plot between the Lidar and the UAV datasets has shown a strong correlation. The comparison of Lidar AGB with UAV leaf-on season has shown R^2 of 0.85 with RMSE of 0.724 Mg/tree. Whereas, UAV leaf-off season has shown R^2 and RMSE of 0.91 and 0.72 Mg/tree respectively. The AGB from UAV and Lidar datasets were found consistent with related some previous studies. Among them (Ni et al., 2019) estimated forest above-ground biomass (AGB) using UAV leaf-on and leaf-off images by taking Lidar as a reference. The result obtained showed that the AGB predicted from UAV images were highly correlated with the Lidar obtained result, and the R^2 was higher than 0.94 and RMSE of lower than 10Mg/ha.

To test the significance of the relationship among UAV and Lidar data t-test, assuming equal variance was conducted. The p-values from the t-test were 0.000378 and 0.077215 for leaf-on and leaf-off seasons. Therefore there was no significant difference observed between the means of Lidar and UAV leaf-off season AGB and the null hypothesis was accepted. But, the p-value for the leaf-on season has shown a significant difference between the two means and the null hypothesis was rejected.

5.4.1. Error propagation

The DTM accuracy assessment between UAV leaf-on and leaf-off, along with Lidar DTM values, has produced a different level of errors. The error was 0.30 and 0.25 meter for both leaf-on and leaf-off seasons, respectively. In terms of percentage, the error was estimated to 25 and 30% for leaf-off and leaf-on seasons, respectively. The two percentage of errors has a difference of 5%, and this variation in DTM has caused a difference in tree height in UAV datasets, and the RMSE error from the two UAV height comparison was 2,1m. The 5% variation from the DTM has propagated to the AGB and caused a difference of 43 Mg/ha. The RMSE error between AGB estimated between UAV leaf-on and the leaf-off season was 0.13Mg/tree.

5.5. Limitations

- Height measurement during the leaf-off season was very challenging because it was challenging to hit the treetop and lead to error result.
- Difficult to identify the dead trees during the leaf-off season.
- Processing UAV and Lidar datasets take a lot of time.
- The weather condition limited me not to gather the expected number of plots.
- Problem to identify the GCPs taken from permanent points while processing the UAV images

6.CONCLUSION AND RECOMMENDATION

6.1. Conclusions

What is the accuracy of DTM obtained from UAV RGB images of leaf-on and leaf-off seasons in comparison to DTM of Lidar data?

Based on the comparison made between Lidar and UAV elevation point, the UAV leaf-on season has produced R^2 and RMSE of 0.72 and 0.3 and 0.8 and 0.25 for the leaf-off season. The UAV leaf-off season has shown a better correlation with Lidar data, and the error was increased as the canopy density increased. From the t-test result, shows no significant difference observed between Lidar and UAV leaf-off season elevation values. However, elevation values derived from UAV leaf-on season was statistically different from Lidar elevation values.

How accurate is the height of the trees derived from UAV RGB images of the leaf-off season compared with the leaf-on season?

The comparison between tree heights of UAV leaf-on and leaf-off season has resulted in R^2 and RMSE of 0.88 and 2.2m, respectively. The computed t-test result showed a significant difference between the two means, and the null hypothesis was rejected.

What is the relationship between CPA derived from UAV images and DBH measured in the field?

The relationship between field-measured DBH and digitized CPA was tested using linear, logarithm, power and quadratic models. The result showed R^2 of 0.76, 0.78, 0.73, and 0.76 with RMSE of 6.78, 6.76, 7.23,6.75 for linear, power, logarithm and quadratic models respectively. Based on the obtained result, the power model used to predict the UAV DBH. The model validation result has shown R^2 of 0.8 with an RMSE of 6.64cm. The model result has shown a positive relationship was observed between biometric DBH and CPA, and the null hypothesis was rejected.

What is the amount of estimated AGB/carbon stock for leaf-off and leaf-on seasons?

The amount of AGB and AGC estimated from UAV leaf-on season were 476 and 223 Mg/ha. While the AGB and AGC derived from the leaf-off season were 519 and 244 Mg/ha. The AGB estimated from the two UAV datasets has a difference of 43Mg/ha.

What is the effect of improved CHM on accuracy result of AGB/carbon stock?

The AGB estimated from the leaf-off season has shown better performance. The comparison between AGB and AGC of UAV leaf-on and leaf-off season has resulted in R^2 of 0.96 with RMSE of 0.13 and 0.06 Mg/tree. According to the t-test, the result obtained, there is no significant difference obtained between the two means. Thus, the null hypothesis is accepted.

According to the comparison made by forest type, the broad-leaf trees has shown R^2 and RMSE of 0.95 and 0.2 Mg/tree. Whereas, the conifer trees has shown R^2 of 0.97 with RMSE 0.15 Mg/tree. Based on the computed t-test result, no significant difference is observed between AGB estimated from leaf-on and the leaf-off season.

How accurate is the AGB derived from UAV RGB images of leaf-on and leaf-off seasons compared to AGB derived from Lidar data?

The accuracy assessment was made between UAV derived AGB compared to Lidar AGB. The comparison between Lidar and UAV leaf-on season AGB has produced R^2 and RMSE of 0.86 and 0.724 Mg/tree. However, the leaf-off has shown higher R^2 of 0.91 with RMSE of 0.72 Mg/tree. According to the obtained result, the AGB from Lidar and UAV leaf-off season has shown a strong positive correlation than the leaf-on season. The result from the t-test showed no significant difference between the two means of Lidar and UAV leaf-off season AGB and the null hypothesis was accepted. But a significant difference was observed in case of the leaf-on season. Therefore, UAV data of leave-off season has proven to be more accurate to assess DTM and consequently the CHM and finally more accurate to assess AGB/AGC.

6.2. Recommendations

I recommend using GCP markers instead of permanent points. Because it was challenging to identify and mark the exact point on the acquired image during image processing, and sometimes caused shifting of points.

Field measurements conducted during the winter season will not be much accurate. This is mainly related to the height measurement with Leica Disto. On the other hand, the shade leaves on the ground will cover some parts of the tree and also affect the height estimation. On top of this, the weather condition by itself affects the quality of the collected data. Its recommended to do it at the end of the summer season.

LIST OF REFERENCES

Anderson, K., & Gaston, K. J. (2013). Lightweight unmanned aerial vehicles will revolutionize spatial ecology. *Frontiers in Ecology and the Environment*, *11*(3), 138–146. https://doi.org/10.1890/120150

Balliett, J. F.(2010). *Oceans: environmental issues, global perspectives*. Cape cod times newspaper

Calders, K., Newnham, G., Burt, A., Murphy, S., Raumonen, P., Herold, M., Kaasalainen, M. (2015). Nondestructive estimates of above-ground biomass using terrestrial laser scanning. *Methods in Ecology and Evolution*, *6*(2), 198–208. https://doi.org/10.1111/2041-210X.12301

Chave, J., Condit, R., Aguilar, S., Hernandez, A., Lao, S., & Perez, R. (2004). Error propagation and sealing for tropical forest biomass estimates. *Philosophical Transactions of the Royal Society B: Biological Sciences*, *359*(1443), 409–420. https://doi.org/10.1098/rstb.2003.1425

Chave, J., Rejou-Mechain, M., Burquez, A., Chidumayo, E., Colgan, M. S., Delitti, W. B. C., … Vieilledent, G. (2014). Improved allometric models to estimate the aboveground biomass of tropical trees. *Global Change Biology*, *20*(10), 3177–3190. https://doi.org/10.1111/gcb.12629

Chukwu, O., Dau, J. H., & Ezenwenyi, J. U. (2017). Crown-Stump Diameter Model for Parkia biglobosa Benth. Species in Makurdi, Benue State, Nigeria. *Journal of Tropical Forestry and Environment*, *7*(1) 43-53 https://doi.org/10.31357/jtfe.v7i1.3021

European Commission. (2003). *Sustainable Forestry and the Europoean Union*. Luxembourg: Office for Official Publications of the European Communities.

Daba, D. E., & Soromessa, T. (2019). The accuracy of species-specific allometric equations for estimating aboveground biomass in tropical moist montane forests: Case study of Albizia grandibracteata and Trichilia dregeana. *Carbon Balance and Management*, *14*(1), 1–13. https://doi.org/10.1186/s13021-019-0134-8

Dandois, J. P., & Ellis, E. C. (2013). High spatial resolution three-dimensional mapping of vegetation spectral dynamics using computer vision. *Remote Sensing of Environment*, *136(*2013*)*, 259–276. https://doi.org/10.1016/j.rse.2013.04.005

de Gouvenain, R. C., & Silander, J. A. (2017). Temperate Forests ☆. In *Reference Module in Life Sciences*. *Reference Module in Life Sciences,* (August), *0-44*https://doi.org/10.1016/b978-0-12-809633-8.02310-4

Dreiss, L. M., & Volin, J. C. (2014). Forests: Temperate Evergreen and Deciduous. *Encyclopedia of Natural Resources: Land*, 1 (October), 214–223. https://doi.org/10.1081/e-enrl-120047447

Effiom, A. E., van Leeuwen, L. M., Nyktas, P., Okojie, J. A., & Erdbrügger, J. (2019). Combining unmanned aerial vehicle and multispectral Pleiades data for tree species identification, a prerequisite for accurate carbon estimation. *Journal of Applied Remote Sensing*, *13*(03), 1. https://doi.org/10.1117/1.jrs.13.034530

Ezenwenyi, J. U., Chukwu, O., & Ike, E. C. (2018). *Modelling Crown Diameter and Canopy Cover Estimation for*

Tectona grandis LINN . F . Plantation in University of Ibadan , Nigeria. (March). https://www.researchgate.net/publication/323747198

FAO. (1999). *Forest Management in Temperate and Boreal Forests : Retrieved from http://www.fao.org/3/a-x4109e.pdf*

Federal Reasearch Centre for Forestry and. (2006). The Condition of Forests in Europe. In *The Condition of forests in Europe*. Retrieved from /http://www.futmon.org/laymans@20report@202011

Frey, J., Kovach, K., Stemmler, S., & Koch, B. (2018). UAV photogrammetry of forests as a vulnerable process. A sensitivity analysis for a structure from motion RGB-image pipeline. *Remote Sensing*, *10*(6), 912 https://doi.org/10.3390/rs10060912

Ganz, S., Käber, Y., & Adler, P. (2019). Measuring tree height with remote sensing-a comparison of photogrammetric and LiDAR data with different field measurements. *Forests*, *10*(8), 694 https://doi.org/10.3390/f10080694

Gatziolis, D., & Andersen, H. E. (2008). A guide to LIDAR data acquisition and processing for the forests of the pacific northwest. *USDA Forest Service - General Technical Report PNW-GTR*, (768), 1–32. https://doi.org/10.2737/pnw-gtr-768

Gibbs, H. K., Brown, S., Niles, J. O., & Foley, J. A. (2007a). Monitoring and estimating tropical forest carbon stocks: Making REDD a reality. *Environmental Research Letters*, *2*(4), 1748-9326 https://doi.org/10.1088/1748-9326/2/4/045023

Gorte, R. W. (2007). Resources , Science , and Industry Division. *Resources Policy*, 1–28. Retrieved from www.crs.gov

Gorte, R. W. (2009). *CRS Report for Congress Carbon Sequestration in Forests Specialist in Natural Resources Policy*.

Gorte, R. W., & Sheikh, P. A. (2010). Deforestation and climate change*. *Deforestation and Climate Change*, 1–54.

Heath, L. S., Kauppi, P. E., Burschel, P., Gregor, H. D., Guderian, R., Kohlmaier, G. H., … Weber, M. (1993). Contribution of temperate forests to the world's carbon budget. *Water, Air, & Soil Pollution*, *70*(1–4), 55–69. https://doi.org/10.1007/BF01104988

Huang, H., He, S., & Chen, C. (2019). Leaf abundance affects tree height estimation derived from UAV images. *Forests*, *10*(10), 931. https://doi.org/10.3390/f10100931

Iizuka, K., Yonehara, T., Itoh, M., & Kosugi, Y. (2018). Estimating Tree Height and Diameter at Breast Height (DBH) from Digital surface models and orthophotos obtained with an unmanned aerial system for a Japanese Cypress (Chamaecyparis obtusa) Forest. *Remote Sensing*, *10*(1), 13. https://doi.org/10.3390/rs10010013

IPCC. (2006). *2006 IPCC guidelines for national greenhouse gas inventories* (S. Eggleston, L. Buendia, K. Miwa, T. Ngara, & K. Tanabe, eds.). Japan: IGES. https://www.ipcc-nggip.iges.or.jp/public/2006gl/

Island, U. H., Above, M., Biomass, G., & Forests, C. P. (2015). *Recent Approaches in Above Ground Biomass Estimation Methods .Plos one* 10(6).*https://doi.org/10.1371/journal.pone.0130143*

Jennings, S. (1999). Assessing forest canopies and understorey illumination: canopy closure, canopy cover and other measures. *Forestry*, *72*(1), 59–74. https://doi.org/10.1093/forestry/72.1.59

Kauffman, J. B., & Donato, D. C. (2012). *W o r k i n g P a P e r Protocols for the measurement, monitoring and reporting of structure, biomass and carbon stocks in mangrove forests*. 1–42. Retrieved from http://citeseerx.ist.psu.edu/viewdoc/download?doi=10.1.1.382.7768&rep=rep1&type

Kebede, B., & Soromessa, T. (2018). Allometric equations for aboveground biomass estimation of Olea europaea L. subsp. cuspidata in Mana Angetu Forest. *Ecosystem Health and Sustainability*, *4*(1), 1–12. https://doi.org/10.1080/20964129.2018.1433951

Krause, S., Sanders, T. G. M., Mund, J. P., & Greve, K. (2019a). UAV-based photogrammetric tree height measurement for intensive forest monitoring. *Remote Sensing*, *11*(7), 1–19. https://doi.org/10.3390/rs11070758

Krause, S., Sanders, T. G. M., Mund, J. P., & Greve, K. (2019b). UAV-based photogrammetric tree height measurement for intensive forest monitoring. *Remote Sensing*, *11*(7), 1–18. https://doi.org/10.3390/rs11070758

Kumar, A., & Sharma, M. P. (2015). Assessment of carbon stocks in forest and its implications on global climate changes. *Journal of Materials and Environmental Science*, *6*(12), 3548–3563.

Kumar, L., & Mutanga, O. (2017). Remote sensing of above-ground biomass. *Remote Sensing*, *9*(9), 1–8. https://doi.org/10.3390/rs9090935

Kustiyanto, E. K. O. (2019). *Estimating Aboveground Biomass / Carbon Stock and Carbon Sequestration using UAV (Unmanned Aerial Vehicle) in Mangrove Forest , Mahakam Delta , Indonesia*. (Masters' thhesis). https://library.itc.utwente.nl/papers_2019/msc/nrm/kustiyanto.pdf

Lal, R., Lorenz, K., Hüttl, R. F., Schneider, B. U., & Von Braun, J. (2012). Recarbonization of the biosphere: Ecosystems and the global carbon cycle. *Recarbonization of the Biosphere: Ecosystems and the Global Carbon Cycle*, (C), 1–559. https://doi.org/10.1007/978-94-007-4159-1

Moudry, V., Gdulová, K., Fogl, M., Klápště, P., Urban, R., Komárek, J., … Solský, M. (2019). Comparison of leaf-off and leaf-on combined UAV imagery and airborne LiDAR for assessment of a post-mining site terrain and vegetation structure: Prospects for monitoring hazards and restoration success. *Applied Geography*, *104*(February), 32–41. https://doi.org/10.1016/j.apgeog.2019.02.002

Musselman, R. C., & Fox, D. G. (1991). A Review of the Role of Temperate Forests in the Global Co2 Balance. *Journal of the Air and Waste Management Association*, *41*(6), 798–807. https://doi.org/10.1080/10473289.1991.10466876

Newton, A., & Featherstone, A. W. (2005). Restoring temperate forests. *Forest Restoration in Landscapes: Beyond Planting Trees*, 320–326. https://doi.org/10.1007/0-387-29112-1_46

Ni, W., Dong, J., Sun, G., Zhang, Z., Pang, Y., Tian, X., … Chen, E. (2019). Synthesis of leaf-on and leaf-offunmanned aerial vehicle (UAV) stereo imagery for the inventory of aboveground biomass of deciduous forests. *Remote Sensing*, *11*(7), 889. https://doi.org/10.3390/RS11070889

Obeng-manu, C. (2019). *Assessing the accuracy of UAV-DTM generated under different forest canopy density and its effect on estimation of aboveground carbon in Asubima forest, Ghana*. Retrieved from https://library.itc.utwente.nl/papers_2019/msc/nrm/obeng-manu.pdf

Paulista, U. E., Em, P. D. E. P., & Biologicas.(2010) .Forests. New York : Taylor & Francis

Pelton, J. N., Madry, S., & Camacho-Lara, S. (2013). Handbook of satellite applications. In *Handbook of Satellite Applications* (Vol. 1–2). https://doi.org/10.1007/978-1-4419-7671-0

Polat, N., & Uysal, M. (2017). DTM generation with UAV based photogrammetric point cloud. *International Archives of the Photogrammetry, Remote Sensing and Spatial Information Sciences - ISPRS Archives*, *42*(4W6), 77–79. https://doi.org/10.5194/isprs-archives-XLII-4-W6-77-2017

Polat, Nizar, & Uysal, M. (2018). An Experimental Analysis of Digital Elevation Models Generated with Lidar Data and UAV Photogrammetry. *Journal of the Indian Society of Remote Sensing*, *46*(7), 1135–1142. https://doi.org/10.1007/s12524-018-0760-8

Potapov, P. (2009). Gross forest cover loss in temperate forests: biome-wide monitoring results using MODIS and Landsat data. *Journal of Applied Remote Sensing*, *3*(1), 033569. https://doi.org/10.1117/1.3283904

Shimano, K. (1997). Analysis of the relationship between DBH and crown projection area using a new model. *Journal of Forest Research*, *2*(4), 237–242. https://doi.org/10.1007/BF02348322

Shrestha, S. K. (2011). *Carbon stock estimation using very high resolution satellite imagery and individual crown segmentation : a case study of broadleaved and needle leaved forest of Dollakha, Nepal*. 48. Retrieved from http://www.itc.nl/library/papers_2011/msc/nrm/shrestha.pdf

Starek, M. J. (2016). Light detection and ranging (Lidar). *Encyclopedia of Earth Sciences Series*, (March), 383. https://doi.org/10.1007/978-94-017-8801-4_244

Stereńczak, K., Zasada, M., & Brach, M. (2013). The accuracy assessment of DTM generated from LIDAR data for forest area - A case study for Scots Pine stands in Poland. *Baltic Forestry*, *19*(2), 252–262. https://link.springer.com/chapter/10.1007/978-3-319-23192-1_53

Vashum, K. (2012). Methods to Estimate Above-Ground Biomass and Carbon Stock in Natural Forests - A Review. *Journal of Ecosystem & Ecography*, *02*(04). https://doi.org/10.4172/2157-7625.1000116

Vankat, J. L. (2002). Boreal and Temperate Forests. *Encyclopedia of Life Sciences*, (March 2002). https://doi.org/10.1038/npg.els.0003738

Wakawa, L. D., & State, Y. (2016). Biomass estimation in forest ecosystems - a review. *Journal of Research in Forestry, Wildlife and Environment*, *8*(2),126-144.https://www.researchgate.net/publication/313402463

Zianis, D., Muukkonen, P., Makipaa, R., & Mencuccini, M. (2005). Biomass and stem volume equations for tree species in Europe. In *Silva Fennica Monographs* (Vol. 4).

Zietara, A. M. (2017). Creating Digital Elevation Model (DEM) based on ground points extracted from classified aerial images obtained from Unmanned Aerial Vehicle (UAV). *Norwegian University of Science and Technology Faculty of Engineering. Department of Civil and Environmental Engineering*, (June), 1–98. http://hdl.handle.net/11250/2452455

APPENDICES

Appendix 1: Filed data collection sheet

Field datasheet

Name of recorder ……………………………………………….. Date (dd/mm/yy) …………………… Plot size radius (m) …………..

Plot no.	Coordinate of plot centre		Elevation (m)	Slope (%)	Hemispherical image code (e.g. P1)
	X:	Y:			

Tree no.	Species:	Tree location		DBH (cm)	Height (m)	Distance from PC (m)	Bearing from PC (degree)	Crown diameter		Remarks
		X	Y					Long. direction (m)	Perp. direction (m)	Isolated (1) Clumped (2)
1										
2										
3										
4										
5										
6										
7										
8										
9										
10										
11										
12										
13										
14										
15										
16										
17										
18										
19										
20										
21										

22										
23										
24										
25										

Appendix 2:GNSS point collection (Permanent points).

Appendix 3: Filed Plot and tree tagging

Appendix 4: Coordinates of tree calculation using distance and bearing.

Finding Coordinate of Points from Distance and Bearing							
ID	Line	Dist. (m)	Bearing in Decimal	Departure L x Sin(Bearing)	Latitude L x Cos(Bearing)	Coordinate	
						Easting	Northing
1						**261623.894**	**476981.148**
2	1-2	7.6	3	0.3978	7.5896	261624.2918	476988.7376
3	2-3	6.3	8	0.8768	6.2387	261625.1685	476994.9763
4	3-4	7.1	44	4.9321	5.1073	261630.1006	477000.0836
5	4-5	4.6	53	3.6737	2.7683	261633.7743	477002.8519
6	5-6	7.7	78	7.5317	1.6009	261641.3061	477004.4529
7	6-7	6.4	80	6.3028	1.1113	261647.6088	477005.5642
8	7-8	2.9	110	2.7251	-0.9919	261650.3340	477004.5723
9	8-9	10.2	130	7.8137	-6.5564	261658.1476	476998.0159
10	9-10	11.7	135	8.2731	-8.2731	261666.4208	476989.7428
11	10-11	6.8	140	4.3710	-5.2091	261670.7917	476984.5337
12	11-12	9.7	158	3.6337	-8.9937	261674.4254	476975.5400
13	12-13	11.1	167	2.4970	-10.8155	261676.9224	476964.7245
14	13-14	8.6	185	-0.7495	-8.5673	261676.1728	476956.1572
15	14-15	4.5	220	-2.8925	-3.4472	261673.2803	476952.7100
16	15-16	9.1	220	-5.8494	-6.9710	261667.4309	476945.7390
17	16-17	9.2	267	-9.1874	-0.4815	261658.2435	476945.2575
18	17-18	9.3	276	-9.2491	0.9721	261648.9945	476946.2296
19	18-19	10.9	313	-7.9718	7.4338	261641.0227	476953.6634
20	19-20	10.2	320	-6.5564	7.8137	261634.4663	476961.4770
21	20-21	9.1	325	-5.2195	7.4543	261629.2467	476968.9313
22	21-22	12.2	321	-7.6777	9.4812	261621.5690	476978.4125
23	22-23	10.8	335	-4.5643	9.7881	261617.0047	476988.2006

Appendix 5: Quality report of UAV leaf-off season image processing.

Summary

Project	last1
Processed	2020-04-06 01:32:04
Camera Model Name(s)	FC330_3.6_4000x3000 (RGB)
Average Ground Sampling Distance (GSD)	4.90 cm / 1.93 in
Area Covered	0.780 km^2 / 77.9534 ha / 0.30 sq. mi. / 192.7268 acres
Time for Initial Processing (without report)	54m:22s

Quality Check

Images	median of 43490 keypoints per image	
Dataset	767 out of 807 images calibrated (95%), all images enabled	
Camera Optimization	0.02% relative difference between initial and optimized internal camera parameters	
Matching	median of 1328.12 matches per calibrated image	
Georeferencing	yes, 3 GCPs (3 3D), mean RMS error = 0.001 m	

Preview

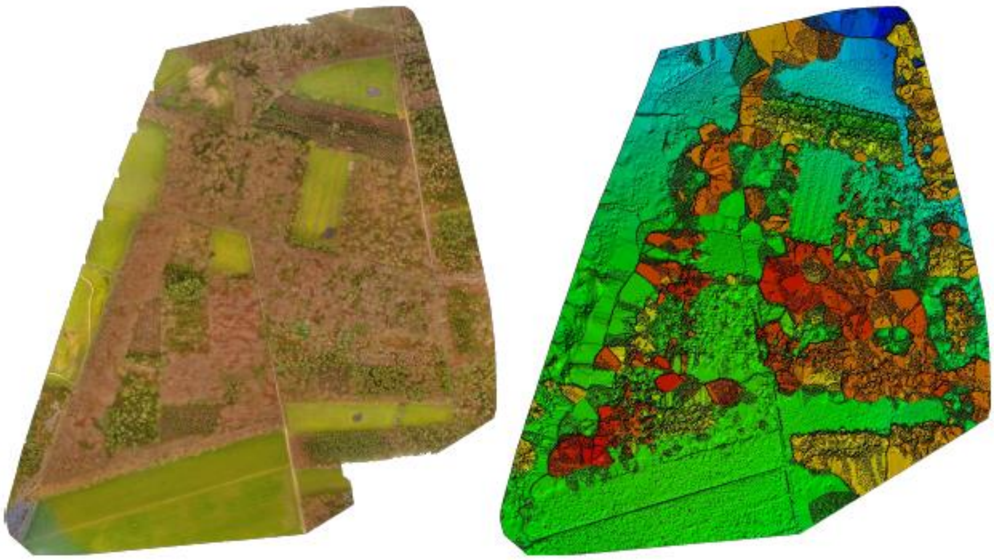

Figure 1: Orthomosaic and the corresponding sparse Digital Surface Model (DSM) before densification.

Appendix 6: Quality report of UAV leaf-off season image processing.

Summary

Project	S_result
Processed	2020-04-04 00:15:14
Camera Model Name(s)	FC330_3.6_4000x3000 (RGB)
Average Ground Sampling Distance (GSD)	4.64 cm / 1.83 in
Area Covered	0.790 km^2 / 79.0145 ha / 0.31 sq. mi. / 195.3501 acres
Time for Initial Processing (without report)	01h:02m:18s

Quality Check

Images	median of 57568 keypoints per image	
Dataset	807 out of 807 images calibrated (100%), all images enabled	
Camera Optimization	0.08% relative difference between initial and optimized internal camera parameters	
Matching	median of 3122.71 matches per calibrated image	
Georeferencing	yes, 3 GCPs (3 3D), mean RMS error = 0 m	

Preview

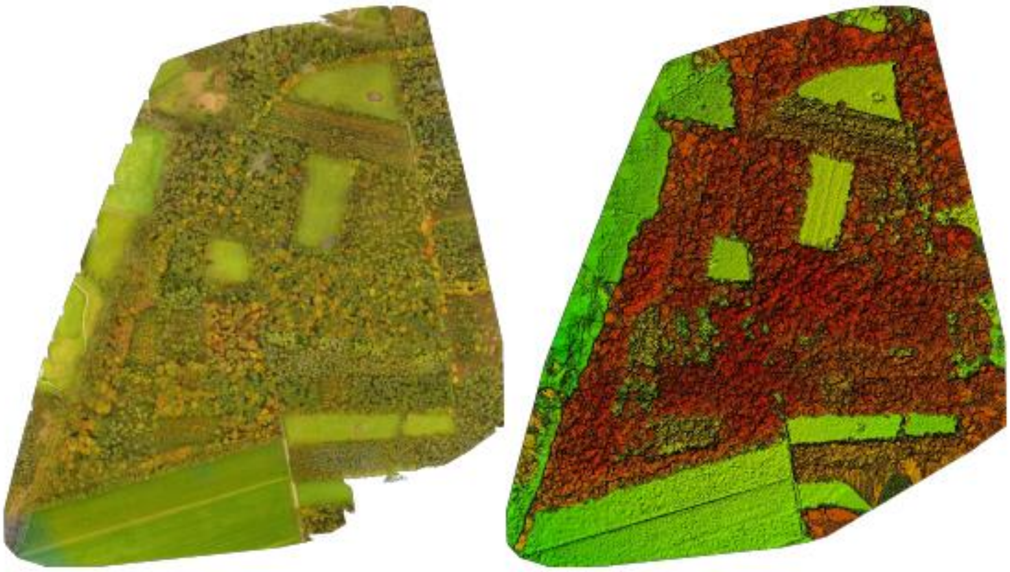

Figure 1: Orthomosaic and the corresponding sparse Digital Surface Model (DSM) before densification.

Appendix 7: Descriptive statistics of Lidar and UAV datasets elevation.

	Lidar	UAV-leaf-off	UAV leaf-0n
Mean	50.40982185	50.33211652	50.25772391
Standard Error	0.035799171	0.050719006	0.049078903
Median	50.49040031	50.44239349	50.39449219
Standard Deviation	0.357991709	0.507190057	0.490789031
Sample Variance	0.128158064	0.257241754	0.240873873
Kurtosis	1.210122438	3.170054163	1.464495753
Skewness	-1.158568399	-1.338067285	-1.265330324
Range	1.741600037	3.29227066	2.282525635
Minimum	49.29589844	48.17724991	48.78993225
Maximum	51.03749847	51.46952057	51.07245789
Sum	5040.982185	5033.211652	5025.772391
Count	100	100	100
Confidence Level(95.0%)	0.071033322	0.100637511	0.097383192

Appendix 8: Lidar and UAV datasets estimated AGB and AGC/plot.

Plot No	AGB/Lidar	AGB/leaf-off Season	AGB/Leaf-on Season	AGC/Lidar	AGC/leaf-off Season	AGC Leaf-on Season
1	14.93424	12.49663175	10.93414521	7.016073	5.873416923	5.13904825
2	13.81199	12.88046689	10.72542697	6.684451	6.053819439	5.040950676
3	11.21633	6.965592547	6.247509405	4.945331	3.273828497	2.93632942
4	14.22224	12.20806749	10.32488599	6.296325	5.737791721	4.852696416
5	23.79594	22.36884225	21.03515546	10.89524	10.51335586	9.886523068
6	18.63885	19.80914831	17.62248111	9.671179	9.310299705	8.282566124
7	25.09377	24.17671465	22.59206793	11.18409	11.36305589	10.61827193
8	19.51745	18.99147527	18.99147527	8.760262	8.925993375	8.925993375
9	23.18137	21.63260096	19.42401756	11.79407	10.16732245	9.129288252
10	17.28135	17.40688678	17.05019446	8.122236	8.181236787	8.013591394
11	14.43971	12.47355639	10.56405274	6.534744	5.862571504	4.96510479
12	10.52198	6.112953979	5.052514217	3.748593	2.87308837	2.374681682
13	22.42154	21.42215463	19.71147329	10.53812	10.06841268	9.264392446
14	7.975731	6.678734547	8.688574428	5.271674	3.139005237	4.083629981
15	15.20855	14.71323365	15.4053825	7.176382	6.915219813	7.240529775
16	21.60484	20.70242546	18.658332	10.15427	9.730139966	8.769416039

17	22.93743	21.44912029	19.75238255	10.78059	10.08108654	9.283619797
18	13.39644	9.881485587	8.235450707	6.786663	4.644298226	3.870661832
19	15.2689	14.01860077	11.63788511	7.019093	6.58874236	5.469806001
20	13.96749	12.25861175	10.12437862	6.56472	5.761547521	4.758457953
21	8.826988	6.370491837	7.256374527	4.148684	2.994131163	3.410496028
22	15.35197	14.62793743	13.31587206	7.148019	6.875130594	6.25845987
23	13.90371	10.37883434	9.529624411	6.853146	4.878052138	4.478923473
24	16.02084	16.22495212	15.20025132	7.678628	7.625727498	7.144118122
25	11.85022	8.754826903	7.390992378	6.491637	4.114768645	3.473766418
26	16.33751	16.88868964	14.92937028	7.470319	7.937684132	7.016804031
27	21.20433	21.12541862	18.88728785	9.966035	9.928946752	8.877025289
28	20.57698	19.01362833	16.90730995	8.622279	8.936405313	7.946435678
29	15.89429	16.16111087	14.89996267	7.529797	7.59572211	7.002982457
30	14.92781	12.76981944	10.93596595	7.215425	6.001815135	5.139903997
31	4.884336	5.506510667	4.781273421	2.295638	2.588060013	2.247198508
32	18.3418	19.43274778	19.43274778	9.173202	9.133391458	9.133391458
33	18.34527	18.60514549	16.68834624	8.620648	8.744418381	7.843522732
34	16.4216	16.60883452	15.61034527	7.71815	7.806152223	7.336862277
35	14.58116	8.100547987	7.53624003	5.569606	3.807257554	3.542032814
Total	**566.905**	**519.2167999**	**476.0797497**	**266.4453**	**244.031896**	**223.7574824**